UNIVERSITÀ POLITECNICA DELLE MARCHE

Advanced technique for detection and removal of pacemakers artifacts from electrocardiographic traces

Enrico Baioni

Master's Thesis in Biomedical Engineering

Supervisor: Prof. Burattini Laura

Advisor: Marta di Pentima

Submission Date: 19/02/2024

I confirm that this sperimental thesis is my own work and I have documented all sources and material used.

Ancona, February 19, 2024 Author Baioni Enrico

Abstract

With the prevalence of cardiovascular diseases on the rise, the global pacemaker market is experiencing significant growth. The market size, valued at USD 5.87 billion in 2023, is projected to reach USD 10.77 billion by 2034, growing at a CAGR of 5.68% during the forecast period. This surge in pacemaker usage reflects the increasing need for advanced cardiac rhythm management and underscores the importance of studies focused on enhancing ECG analysis in the presence of pacemakers. In response to this growing demand for pacemaker technologies, the project focuses on the development of advanced algorithms for the detection and removal of pacemaker pulses from ECG traces. These algorithms are essential for improving the accuracy of ECG analysis, especially in patients with pacemakers, where standard interpretation techniques may be confounded by the artificial signals generated by the device. Addressing the complex challenge of pacemaker pulse detection in ECG traces, the project developed two distinct algorithms. Addressing the complex challenge of pacemaker pulse detection in ECG traces, the project developed two distinct algorithms. The first algorithm, building upon established techniques, demonstrated efficacy in identifying PM pulses in clear ECG traces but encountered difficulties in the presence of noise. To overcome this, the second algorithm was crafted, harnessing the unique rising edge characteristic of PM pulses. This innovative approach proved successful in both noise-free and noisy conditions, significantly enhancing the ability to detect arrhythmias in scenarios where conventional arrhythmia detection software was ineffective. This advancement paved the way for the introduction of the ”Flattening Method” and the ”Interpolation Method” – two approaches aimed at isolating and removing PM pulses from ECG traces, thereby improving the clarity and reliability of cardiac rhythm analysis in clinical practice. The Flattened Method, a simpler technique, involved flattening the PM pulse to the baseline level, effectively neutralizing its impact on the ECG waveform. However, this method did not preserve the natural ECG morphology. The Interpolation Method, on the other hand, employed linear regression and spline interpolation. This approach initially replaced the PM pulse with a straight line connecting its highest and lowest points, followed by spline interpolation. This method successfully maintained the continuity and natural pattern of the ECG waveform.

The validation of the algorithms across different frequencies revealed significant insights into their performance. Testing at higher frequencies, specifically 128 kHz and 64 kHz, yielded excellent results, with the algorithms achieving near-perfect detection rates. At these frequencies, sensitivity (Se) and positive predictive value (PPV) both reached 100%, indicating exceptional accuracy in PM pulse detection and removal. In contrast, at lower

frequencies such as 32 kHz, 16 kHz, 8 kHz, and 4 kHz, the algorithms' performance decreased, with both sensitivity (Se) and positive predictive value (PPV) values declining notably. For instance, at 32 kHz, Se remained high at 100% while PPV slightly decreased to 97.50%. However, at 16 kHz, Se slightly decreased to 99.97% and PPV more substantially to 80.25%. The decrease was more pronounced at 8 kHz, with Se dropping to 97.37% and PPV to 18.29%, and at 4 kHz, Se further decreased to 80.66% with PPV falling to a mere 1.56%. This drop in accuracy at lower frequencies is attributed to the increased distortion of PM pulses, highlighting the importance of high sampling rates in achieving reliable and precise ECG analysis. The choice of different frequencies for testing reflects a comprehensive approach to assess the algorithms' efficacy under varying conditions, ensuring their robustness and adaptability in real-world scenarios

For future research, the focus will be on refining these algorithms to further enhance ECG analysis in the presence of pacemakers. This includes developing algorithms with adaptive window sizes that adjust according to the characteristics of each PM pulse, ensuring more precise removal. Additionally, testing these algorithms with actual patient data will be crucial in evaluating their performance in real-world clinical settings. Finally, integrating these advanced algorithms into existing clinical ECG analysis software will be a significant step towards improving cardiac care for patients with pacemakers. This integration will enable more accurate and reliable diagnosis of cardiac conditions, ultimately contributing to better patient outcomes.

Contents

Chapter 1

Introduction

The global pacemaker market is undergoing substantial growth, reflecting an increased reliance on these devices in modern cardiology. In 2023, the market was valued at USD 5.87 billion, and it is projected to nearly double, reaching USD 10.77 billion by 2034. This remarkable growth, with a compound annual growth rate (CAGR) of 5.68%, is primarily driven by the escalating prevalence of cardiovascular diseases (CVDs) and the rising costs associated with managing heart conditions. The surge in pacemaker usage underscores the critical importance of advancements in pacemaker technologies and their integration into cardiac care. This trend is further illustrated by the expected increase in the number of pacemakers globally. As of 2016, approximately 1.14 million pacemakers were in use worldwide. By 2023, this figure is anticipated to rise to 1.43 million units. This increase highlights the vital role pacemakers play as a life-saving implantable medical device for individuals with specific heart conditions, including arrhythmias, congenital heart disease, and age-related heart muscle deterioration. With heart disease being the leading cause of death globally, the demand for pacemakers is rising not only in developed countries but also in middle- and low-income countries, where heart diseases are becoming more prevalent(1).

The pacemaker market's growth reflects the broader expansion of the global cardiac device market, with varying access to pacemakers worldwide. The United States, Germany, and Japan hold the largest regional shares in the global medical device industry sales. However, affordability remains a major concern for many patients globally, affecting access

to these crucial cardiac devices. The burgeoning pacemaker market, indicative of the increasing reliance on these devices in cardiology, is directly linked to the critical role of the heart in the circulatory system. The heart's precise rhythm, essential for efficient blood circulation, can sometimes be disrupted by conditions that affect its electrical conduction system. In such cases, pacemakers play a vital role in restoring and maintaining rhythmic harmony. As the market for these devices grows, driven by the escalating prevalence of cardiovascular diseases, the necessity for advanced pacemaker technologies becomes more evident. These devices, integral to modern cardiac care, help in managing rhythm disorders, thereby safeguarding the heart's essential function in the circulatory system. This connection highlights the importance of pacemakers in contemporary cardiology and sets the stage for a deeper exploration into heart anatomy and the innovative solutions provided by pacemaker technology. The heart, a pivotal organ in the circulatory system, is designed for rhythmic and efficient blood pumping, ensuring the circulation of oxygen-rich blood throughout the body [2]. The rhythmic contractions of the heart are orchestrated by an intricate electrical conduction system, often referred to as the cardiac conduction system. This system includes a specialized group of cells known as the sinoatrial (SA) node, located in the right atrium, and the atrioventricular (AV) node, positioned near the atrial-ventricular septum. These nodes generate electrical impulses that travel through the heart, signaling the muscle cells to contract in a coordinated sequence. The SA node, often referred to as the heart's natural pacemaker, initiates each heartbeat by sending an electrical signal that causes the atria to contract, pushing blood into the ventricles. The electrical impulse then travels to the AV node, where it is briefly delayed, ensuring that the ventricles have adequate time to fill with blood. Subsequently, the signal travels along specialized pathways called the bundle of His and Purkinje fibers, stimulating the ventricles to contract and pump blood to the lungs and the rest of the body. While the heart's natural pacemaker system is highly effective, it can sometimes malfunction or become impaired due to various medical conditions or aging. This rhythm can be disrupted by various conditions, leading to arrhythmias where the heart beats too slowly, too quickly, or irregularly, which may lead to serious health complications or even life-threatening situations. In these cases, pacemakers become crucial. They are small electronic devices implanted to moni-

tor and regulate the heart's rhythm. By delivering electrical impulses, pacemakers help maintain an adequate heart rate, ensuring efficient blood circulation. They are available in different types, such as single-chamber and dual-chamber pacemakers, to address specific cardiac conditions. The role of pacemakers is vital in modern cardiology, offering life-saving solutions to those with rhythm disorders and significantly improving patient outcomes. Within this context, the importance of pacemakers in contemporary cardiology becomes evident. Pacemakers are small electronic devices implanted in the chest or abdomen that are designed to monitor and regulate the heart's rhythm. They function by delivering electrical impulses to the heart muscle when it fails to beat at an appropriate rate or rhythm. This ensures that the heart continues to pump blood efficiently, maintaining oxygen delivery to vital organs and tissues. Pacemakers come in various types, each designed to address specific cardiac issues. Single-chamber pacemakers, for example, regulate either the atria or ventricles, while dual-chamber pacemakers synchronize the activity of both atria and ventricles, mimicking the natural coordination of the heart [3]. Understanding the anatomy and electrical conduction system of the heart is fundamental to comprehending the crucial role of pacemakers in maintaining cardiac rhythm. These remarkable devices have revolutionized the field of cardiology, offering life-saving solutions to individuals with arrhythmias, ensuring the heart's harmonious rhythm, and ultimately improving the quality of life for countless patients worldwide. The artificial pacemaker is a compact electromedical device, typically measuring just a few centimeters (around 6 or 7). It emits controlled electrical impulses designed to stimulate or regulate the heartbeat. Pacemakers are implanted when the heart's natural electrical conduction system, particularly the sinoatrial node, can no longer maintain its normal function. Heart rates that are too slow or too fast can compromise the heart's ability to effectively pump blood, leading to serious issues. The pacemaker comprises electronic circuitry powered by a sealed battery enclosed in a titanium casing. It is surgically placed just beneath the skin in the chest, near the heart. To transmit the electrical impulses to the heart's chambers, the pacemaker is equipped with specialized wires, often referred to as electrodes or leads. Pacemakers can serve both temporary and permanent purposes. Temporary use might stabilize the heartbeat after a traumatic event like a heart attack, while permanent im-

plantation is necessary when the heart cannot naturally maintain a proper rhythm. The most common reason for implanting an artificial pacemaker is bradycardia, a condition characterized by an abnormally slow heart rate. This condition can lead to reduced blood flow and insufficient oxygenation of tissues, resulting in various health problems. However, there are various pathological reasons that may necessitate pacemaker implantation, as we shall explore further. In the field of pacemakers, continuous innovations are being made. To provide a brief historical overview, the concept of pacemakers traces its origins back to 1958, but significant progress was made in the following years. Engineer Greatnatch and cardiologist Chardack developed the first fully implantable pacemaker in 1959 [4]. It could effectively treat patients with atrioventricular block (AV block) by stimulating the ventricle. Greatnatch's groundbreaking discovery came about somewhat accidentally in 1956 while working with a cardiac rhythm recorder. He inadvertently added an incorrect electronic component, causing the device to produce electrical impulses instead of merely recording them. Realizing the potential, he miniaturized and packaged the device over the next two years, culminating in a successful demonstration in a dog in May 1958 [4]. In 1960, the pacemaker was implanted in the first human patient, a 77-year-old man who continued to live for another 18 months. Initially, these pacemakers used mercury-zinc batteries, which were prone to many failures. Later, biological and nuclear batteries were experimented with. However, since 1972, most pacemakers have used lithium-iodine batteries, known for their high energy density and longevity (lasting more than 10 years). These early pacemakers operated at a fixed rate or asynchronous, continuously stimulating the heart without considering its natural electrical activity. This sometimes led to arrhythmias or ventricular fibrillation. To address this issue, a sense amplifier was added to recognize the heart's natural electrical activity, allowing the pacemaker to activate only when necessary. This innovation gave rise to demand pacemakers, capable of electrically stimulating the heart only in the absence of its natural rhythm. Demand pacemakers paved the way for modern pacemakers, equipped with leads that serve both pacing and sensing functions in the heart's chambers. In 1970, dual-chamber pacemakers were introduced, capable of sensing cardiac activity in both the atrium and ventricle to determine if stimulation is needed. These devices are commonly used for patients with sinoatrial node disease [4].

While demand pacemakers satisfied certain physiological demands, they couldn't adapt to the body's needs during stress or physical activity. The latest innovations in pacemakers, introduced in the 1980s, involve rate-responsive pacemakers, which adjust the pacing rate based on physiological or physical parameters, such as body movement, respiratory rate, blood pH, blood temperature, minute ventilation, central venous temperature, intracardiac ventricular impedance, and more. Sensors detect these parameters and convert them into electrical signals to regulate the pacemaker's pacing rate, overcoming chronotropic incompetence in patients. In 2013, a significant milestone was achieved with the development of the wireless pacemaker, the first of its kind. This pacemaker, comprising a small battery, is implanted directly into the ventricle through the femoral vein without the need for leads. This approach reduces the risk of infection associated with traditional pacemaker implantation. Moreover, the battery life significantly surpasses traditional pacemakers, ranging from 9 to 17 years compared to 5-8 years. The implantation procedure is quick, averaging about 28 minutes. However, it's important to note that this wireless pacemaker is currently limited to patients who require ventricular stimulation. In summary, pacemakers have a rich history of development, from their early beginnings in the late 1950s to the cutting-edge innovations of today, such as rate-responsive pacemakers and wireless technology [4]. These devices have greatly improved the quality of life for individuals with cardiac conduction disorders, ensuring the heart's rhythm remains in sync with the body's needs. This ongoing evolution in pacemaker technology continues to shape the field of cardiology and offer hope to patients with arrhythmia and other heart conditions.

Amidst the ongoing advancements in pacemaker technology, including the development of wireless pacemakers and rate-responsive systems, arises a significant challenge in cardiac electrophysiology: the accurate analysis of ECG signals in patients with pacemakers. This challenge forms the crux of the current research project. The aim is to develop sophisticated algorithms capable of effectively detecting and removing pacemaker pulses from ECG traces, thereby enhancing the accuracy of cardiac rhythm analysis. This endeavor addresses a critical need in cardiology, ensuring that ECG interpretation remains reliable and precise, even in the presence of artificial pacemaker signals. The project seeks not only to innovate in the realm of ECG analysis but also to contribute to the broader goal of im-

proving cardiac care for patients with pacemakers.

Chapter 2

Heart physiology and ECG Characteristics

The heart is an intricate muscular organ that resides within the thoracic cavity, encapsulated by the pericardium. It is composed of four chambers - two atria and two ventricles - strategically positioned to facilitate the efficient flow of blood through the circulatory system. The four chambers beat normally in a synchronous manner: Firstly, the atrial contraction (atrial systole), then the ventricular contraction (ventricular systole). During the diastolic phase all the chambers are relaxed. The right atrium receives deoxygenated blood from the systemic circulation via the superior and inferior vena cavae, while the left atrium receives oxygenated blood from the pulmonary veins, enabling the heart to function as a muscular pump, propelling blood through the pulmonary and systemic circulations [5].

Further augmenting this intricate system is the coronary circulation, a network of blood vessels that supplies the myocardium with essential nutrients and oxygen. The coronary arteries, emanating from the aorta, intricately traverse the heart's surface, culminating in anastomotic capillary beds that facilitate the exchange of vital substances. The anatomical entities constituting the cardiac conduction system encompass the sinoatrial node (SA node), the interatrial pathways, the atrioventricular node (AV node), the bundle of His along with its ramifications, and the Purkinje network. These discrete elements of the conduction system exhibit inherent capabilities for autonomous discharge. However, it is

noteworthy that the SA node typically manifests a swifter rate of discharge in comparison to its counterparts [5]. This phenomenon involves the emanation of depolarization from the SA node to adjacent regions prior to its self-termination. Hence, the sinoatrial node assumes the crucial role of the endogenous cardiac pacemaker, with its discharge frequency dictating the timing of cardiac pulsations.

In marked contrast to skeletal musculature, which is subject to conscious control via the central nervous system, the heart possesses/holds self-sufficiency. It possesses an intrinsic stimulatory apparatus that gives rise to the electrical impulse governing cardiac contraction. This stimulus, which serves as the trigger for contraction, possesses an electrical nature and arises involuntarily from regulatory centers within the central nervous system, localized in the cerebral and spinal regions. Subsequently, this impulse is transmitted from the central nervous system to the heart through both parasympathetic and sympathetic efferent conduits. Termed the sinoatrial node, this stimulatory locus generates the neural impulse, similar to an electric surge, which serves as the catalyst for cardiac contraction. This innate attribute, denominated automatism, empowers it to spontaneously generate the stimulus governing heart rate (referred to as sinus rhythm), thereby substantiating its role as the authentic 'pacemaker' of the heart. Situated proximal to the opening of the superior vena cava within the right atrium, the sinoatrial node occupies a pivotal anatomical locale [5].

The human heart's functionality is governed by its intricate conduction system, responsible for initiating and coordinating the electrical impulses that trigger cardiac contractions. This system begins with the sinoatrial (SA) node, the heart's natural pacemaker, which generates electrical impulses that prompt the atria to contract. The impulses then travel to the atrioventricular (AV) node, where they are briefly delayed, allowing the ventricles time to fill with blood. Following this, the impulses move through the His-Purkinje network, leading to the synchronized contraction of the ventricles. This orchestrated sequence of events ensures efficient pumping of blood throughout the body [6], as shown in Figure 2.1.

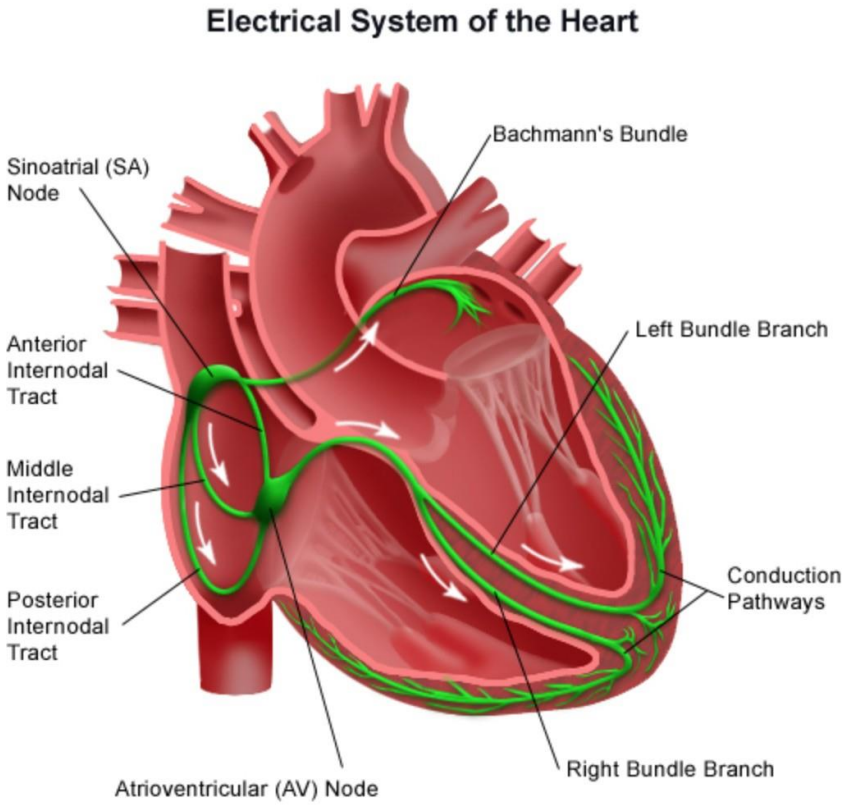

Figure 2.1: Heart's conduction system

The contraction of cardiac muscle cells, which expels blood, is triggered by propagating action potentials along their membranes. The heart's rhythmic contractions stem from spontaneously generated action potentials, a property termed autorhythmicity.

There are two distinct types of cardiac muscle cells: the **contractile cells**, constituting 99 of cardiac muscle, responsible for mechanical pumping, and the **autorhythmic cells**, specialized in initiating and conducting action potentials that drive contractile cell contraction. In contrast to autorhythmic cells, the membrane of contractile cells remains at a resting potential of around -90 mV until stimulated by electrical activity emanating from the pacemaker. The action potential of each heart muscle cell is characterized by swift depolarization, a plateau phase, and a leisurely repolarization process. Autorhythmic cells lack a resting potential but exhibit pacemaker activity. Their membrane potential gradually depolarizes between consecutive action potentials until the threshold potential triggers a new action potential. Through repeated cycles of depolarization and discharge, these

cells cyclically initiate action potentials that propagate throughout the heart, orchestrating rhythmic contractions without neural prompting.

Various ionic mechanisms govern the pacemaker potential, involving potassium (K+) channels in the initial phase and T-type calcium (Ca2+) channels later on. After reaching the threshold potential, the rising phase of the action potential is driven by the opening of long-lasting (L-type) calcium channels, producing the characteristic impulse. The descending phase, as customary, results from potassium channel activation. The collective electrical activity of all cardiac muscle fibers, recorded extracellularly, culminates in the Electrocardiogram (ECG) [7].

2.1 Electrocardiogram (ECG) features

The electrocardiogram (ECG) is a vital tool in cardiac diagnostics, reflecting the electrical activities of the heart through various waveforms and intervals. The ECG's complexity lies in its ability to capture the cumulative action potentials of myocardial fibers, translating these into visible and measurable patterns. The conductive nature of bodily fluids facilitates this extracellular recording, allowing for the detailed observation of potential shifts throughout the cardiac cycle.

As shown in Figure 2.1, each segment and wave of the ECG correlates with specific cardiac activities [8][9]:

- The **P wave** represents atrial depolarization. Its normal parameters include a height not exceeding 2.5 mm and a width within 0.11 seconds.
- The **QRS complex** signifies ventricular depolarization. The initial negative deflection post-P wave, the Q wave, typically does not exceed 0.03 seconds, reflecting ventricular septal depolarization. The R wave, as the first positive deflection post-P wave, denotes the depolarization of the ventricular mass, while the S wave, a negative deflection following the R wave, indicates later stages of ventricular depolarization. Notably, subsequent positive and negative deflections are labeled R' and S',

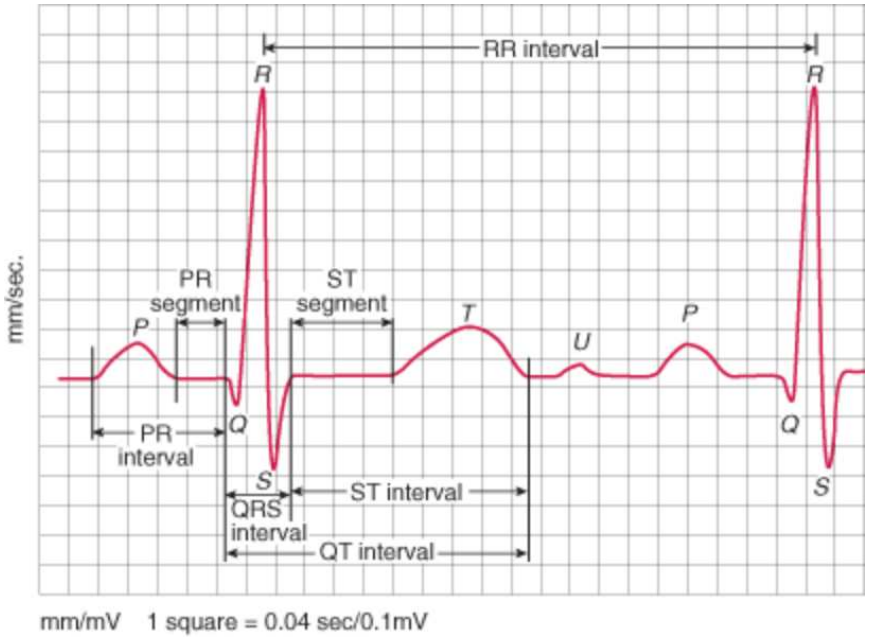

Figure 2.2: Classic example of ventricular extrasystole, characterized by an early and aberrant QRS complex, distinct from the regular cardiac rhythm.

respectively.

- The **T wave** represents ventricular repolarization and can be either positive or negative, following the QRS complex. Its area and polarity generally mirror those of the main QRS component.
- Occasionally, the **U wave** follows the T wave, generally matching its polarity. Its exact origin remains speculative, potentially representing repolarization of papillary muscles or afterpotentials.

The ECG also features critical intervals and segments:

- The **PR interval**, spanning from the onset of the P wave to the beginning of the QRS complex, indicates the time required for atrial depolarization and conduction through the AV node and bundle branches.
- The **QRS interval**, covering the Q wave to the end of the S wave, encompasses ventricular depolarization.

- The **QT interval** extends from the Q wave's start to the T wave's end, including both ventricular depolarization and repolarization phases.
- The **PR segment** and **ST segment** denote the recording between the P wave's end and the QRS complex's start, and from the end of ventricular depolarization to the T wave's onset, respectively.

It is within these parameters that abnormalities indicative of arrhythmias can be detected. For instance, SA block presents as an irregular rhythm with pauses, whereas various degrees of AV block manifest as alterations in the PR interval or complete dissociation between P waves and QRS complexes. The presence of premature ventricular contractions in ventricular extrasystole is apparent through aberrant QRS complexes, as demonstrated in Figure 2.2. This image exemplifies the distinct morphology of ventricular extrasystole, highlighting the aberrant QRS complex characteristic of this arrhythmia. Bundle branch blocks and conditions like atrial flutter and fibrillation also exhibit distinct ECG patterns. These deviations, especially critical in patients with pacemakers, underscore the importance of ECG interpretation in cardiac care, forming the cornerstone of effective diagnosis and management.

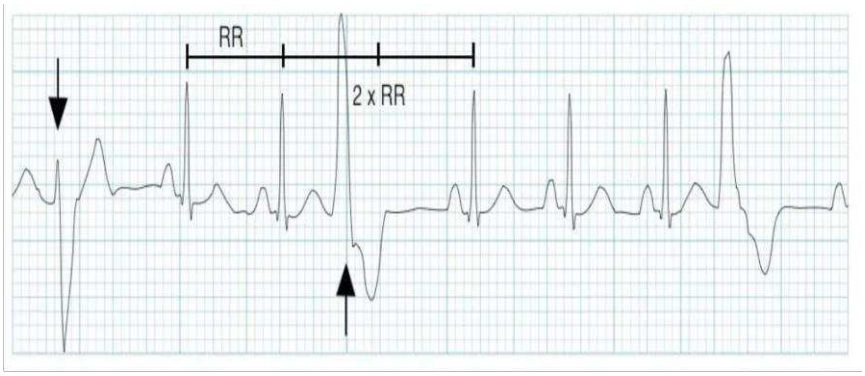

Figure 2.3: Characteristics of a normal ECG

Chapter 3

Pacemaker characteristics

The realm of cardiac rhythm management has been revolutionized by the advent of pacemaker technology. These devices are not mere novelties of medical engineering; they are essential lifelines for patients with arrhythmias, providing a synthetic cadence to hearts with irregular rhythms. A pacemaker's capability hinges on its characteristics, which are fine-tuned to meet the diverse needs of the cardiac tissues they serve.

At their core, pacemakers are sophisticated electronic apparatuses designed to monitor and correct the cardiac rhythm. They achieve this through a series of internal algorithms that adapt to the patient's physiological signals, ensuring that the heart maintains an appropriate rate and rhythm. The characteristics of these devices encompass a broad range of functionalities—from basic pacing in cases of bradycardia to more complex modalities for managing atrial fibrillation or heart failure.

Pacemakers are defined by their ability to sense intrinsic cardiac activity and deliver electrical impulses when necessary. This dual function of sensing and pacing is central to their operation. They are equipped with leads, or electrodes, that are placed in contact with the heart muscle, allowing for the delivery of electrical stimuli and the detection of the heart's own electrical activity.

Further, pacemakers come with programmable settings that enable customization for individual patient needs. These settings determine the device's responsiveness and include features such as rate responsiveness, which allows the device to adjust the pacing rate based on the patient's activity level, and mode switching, which enables the device to

change its pacing strategy in the presence of arrhythmias.

The longevity and reliability of pacemakers are also key characteristics, with battery life and lead integrity being primary concerns. Advances in battery technology and lead design have significantly extended the service life of these devices, reducing the frequency of surgical interventions for replacements or repairs [10].

In the subsequent section on modalities and types, we will delve into the specific pacing modes and configurations available in modern pacemakers. This will include an exploration of single-chamber, dual-chamber, and biventricular pacing, each tailored for specific clinical scenarios, and how these modalities enhance the therapeutic capabilities of pacemakers.

.

3.1 Systems, types and modalities

Pacemakers are integral to the management of cardiac arrhythmias, offering life-sustaining therapy to patients with rhythm disorders. With advancements in technology, the types and systems of pacemakers have evolved to address a broad spectrum of clinical needs. This section outlines the primary categories of pacemakers and their respective modalities.

Pacemaker systems are generally comprised of pulse generators and electrodes. Pulse generators are the command centers that produce the necessary electrical activity, typically placed in the infraclavicular region. Electrodes, or leads, are responsible for delivering this activity to the heart's musculature.

There are three fundamental types of pacemakers [11]:

- **Single Chamber Pacemakers**: These are connected to a single chamber of the heart, either the atrium or the ventricle. They are simpler in design and suitable for patients requiring basic pacing needs.
- **Dual Chamber Pacemakers**: Equipped with leads in both the atrium and ventricle, they offer more synchronized pacing. This type is beneficial for patients needing coordinated atrioventricular pacing.

- **Biventricular Pacemakers**: Utilized in cardiac resynchronization therapy, they are sophisticated systems that pace both ventricles simultaneously to optimize cardiac function, especially in the context of heart failure.

The modes of pacemaker operation are defined by a standardized code known as the NBG code (figure3.1), which encapsulates the pacemaker's function across five domains:

- **Chamber Paced**: Indicates which chamber of the heart the pacemaker is stimulating (e.g., atrium, ventricle, or both).
- **Chamber Sensed**: Refers to the chamber where the pacemaker detects the heart's intrinsic electrical activity.
- **Response to Sensing**: This aspect dictates how the pacemaker responds to the sensed intrinsic cardiac events, like inhibiting or triggering pacing.
- **Programmability**: This feature allows the pacemaker's settings to be adjusted, such as pacing rate or output, adapting to the patient's changing needs.
- **Rate Modulation**: Also known as rate responsiveness, it allows the pacemaker to adjust its pacing rate based on the physiological demands of the patient, such as during exercise.

Position I	Position II	Position III	Position IV	Position V
Pacing Chamber(s)	Sensing Chamber(s)	Response(s) to Sensing	Programmability	Anti-Tachycardia Function(s)
O= None	O= None	O= None	O= None	O= None
A = Atrium	A = Atrium	I = Inhibited	P = Programmable	P = Pacing
V = Ventricle	V = Ventricle	T = Triggered	M= Multiprogrammable	S = Shock
D = Dual (A+V)	D = Dual (A+V)	D = Dual (I+T)	C = Communicating	D = Dual (P+S)
			R = Rate Modulation	

Figure 3.1: Identification code defining the pacemakers modalities.

The NBG code, a systematic representation of pacemaker functionalities, categorically defines the operational modes that dictate how these devices interact with a patient's intrinsic cardiac activity. Each mode, encapsulated in this code, is tailored to address specific cardiac rhythm management needs, with varying strategies employed particularly in single and dual chamber pacemakers.

In single chamber modes, the pacemaker either exclusively paces (Ventricular Pacing - **VOO**) or paces and senses the ventricle (Ventricular Inhibited Pacing - **VVI**), inhibiting pacing when intrinsic activity is detected. The **VVI** mode, for instance, ensures that the pacemaker only intervenes when the heart's natural rhythm is slower than the programmed rate, thereby avoiding unnecessary pacing.

Dual chamber modes, on the other hand, are more complex. They not only pace and sense both chambers but also maintain atrioventricular (AV) synchrony. The Dual Chamber Pacing (**DDD**) mode, a versatile setting, adapts to the heart's intrinsic rhythms. It maintains the coordination between atrial and ventricular contractions, crucial for patients requiring support in both chambers. This mode represents a significant advancement over single chamber modes, as it can respond more naturally to the varying demands of the cardiac cycle.

However, it's important to note that asynchronous modalities, such as **AOO** (Atrial Pacing) or **VOO**, are less commonly used in current clinical practice. Asynchronous pacing lacks the ability to sense the heart's own electrical activity and can potentially pace at inappropriate times, leading to what is known as 'pacemaker syndrome' or, in more serious cases, the risk of inducing arrhythmias like pacemaker-mediated tachycardia. With the advent of advanced sensing technologies, pacemakers can now more accurately detect intrinsic cardiac activity, allowing for synchronous pacing modes (like **DDD** or **VVI**) that are more physiologically appropriate and reduce the risk of such complications[11][12].

3.2 Pattern stimulation characteristics

The exploration of pacemaker stimulation patterns represents a crucial aspect in the advancement of cardiac rhythm management. It delves into the realm where intricate engineering meets clinical necessity, culminating in devices that are both life-sustaining and technologically sophisticated. The focus here is not just on the stimulation patterns themselves, but also on how they align with established European normative and compare with the characteristics of pacemakers available in the market.

Pacemakers, engineered to correct or manage heart rhythm disorders, function by delivering precisely timed electrical impulses. These impulses, or stimulation patterns, are at the heart of pacemaker functionality. They are designed to mimic the heart's natural rhythm, adapting to the patient's varying needs, and to maintain an adequate heart rate, either by replacing the natural cardiac pacemaker in cases where it is deficient or by supporting the intrinsic heart rhythm when it falters. To achieve this, pacemakers use stimulation patterns that are tailored to individual patient needs. These patterns vary in terms of pulse amplitude, frequency, duration, and waveform, parameters that are determined based on the underlying cardiac condition, the patient's physiological demands, and the specific characteristics of the pacemaker lead and electrode.

A critical component of this exploration is the examination of these stimulation patterns against the backdrop of the International Electrotechnical Commission (IEC) standards [13]. These standards, representing the cornerstone of safety and effectiveness in medical device technology, provide a framework against which pacemaker designs are measured and evaluated. The analysis in subsequent sections will delve into how these patterns adhere to the stringent requirements set forth by these normatives, highlighting areas of compliance and divergence.

Simultaneously, a comparative analysis with commercially available pacemakers. This comparison is pivotal in understanding the real-world application of the IEC standards and in assessing the diversity and innovation in pacemaker technology present in the market. By evaluating various commercial models, the study sheds light on the spectrum of stimulation patterns utilized, offering insights into their design philosophies and operational

nuances.

3.2.1 Stimulation impulse simulating pacemaker according to the normative

The characterization of pacemaker stimulation patterns, as defined by the relevant European normatives, focuses primarily on specific, quantifiable characteristics of the pacemaker (PM) pulse. These characteristics include amplitude, pulse duration, and the duration of the rising edge. Understanding these specifications is crucial for both the design of pacemakers and the development of algorithms for detecting and analyzing PM pulses in ECG traces [13].

- **Amplitude**: According to the normatives, a PM artifact is identified based on its amplitude, which ranges from 2 to 700 millivolts (mV). This wide range accommodates various types of pacemakers and patient-specific settings. The amplitude of a PM pulse is significant as it determines the electrical impulse strength delivered to the heart tissue. In clinical practice, the amplitude is adjusted based on individual patient requirements to ensure effective cardiac pacing while minimizing power consumption and prolonging device longevity.

- **Pulse Duration (PD)**: The pulse duration of a pacemaker artifact, as stipulated by the normatives, falls within the range of 0.5 to 2 milliseconds (ms), is defined as the interval from the start of the rising edge to the end of the trailing edge of the pulse. This duration is critical as it represents the time during which the pacemaker delivers the electrical stimulus to the heart. It is important to note that this duration does not include the recharge phase of the pulse, which is part of the pacemaker's overall cycle but is not directly involved in cardiac stimulation.

- **Rising Edge Duration**: The normatives specify that the rising edge of the PM pulse should be less than 0.1 ms. The rising edge is the initial phase of the pulse where the voltage rapidly increases. A shorter rising edge duration is essential for the

prompt and efficient delivery of the stimulus to the heart tissue. It ensures that the electrical impulse is sharp and distinct, which is particularly important for accurate detection and analysis in ECG readings.

These parameters – amplitude, pulse duration, and rising edge duration – are essential in defining what constitutes a pacemaker pulse. They serve as standard guidelines for pacemaker manufacturers and also provide a basis for healthcare professionals and researchers to identify and interpret PM pulses in clinical and research settings. In subsequent sections, the discussion will extend to how these normative-defined characteristics compare to those observed in pacemakers available on the market, providing a comprehensive understanding of pacemaker stimulation patterns in both theoretical and practical contexts.
The image provided below (figure 3.1) shows two representations of a pacemaker (PM) impulse: Figure A illustrates an ideal impulse, while Figure B shows a more realistic depiction. In an ideal scenario (A), the impulse is characterized by a uniform amplitude and a sharp, clear onset and offset, represented by the rising and trailing edges within a specified pulse duration. In contrast, Figure B captures the complexities of a real-world PM impulse. Four primary phases characterizes pacemaker impulse:

- **Rising edge**: It refers to the initial phase of the electrical signal generated by the pacemaker to stimulate the heart. This phase is characterized by a rapid increase in voltage from a baseline level to a peak, marking the onset of the pacemaker's pacing pulse.

- **Capacitive Drop**: This is observed at the onset of the pulse. It is a phenomenon where the initial voltage spike drops rapidly before stabilizing. This effect is due to the capacitive properties of the heart tissue and the lead-tissue interface. When the pacemaker pulse is applied, the capacitors (in this case, the tissue and pacemaker lead interface) initially resist the change in voltage, causing a temporary drop in the observed amplitude before it reaches a steady state. This capacitive drop reflects the transient behavior of the cardiac cells and pacemaker circuitry as they interact electrically.

- **Trailing edge**: As the pacemaker delivers a pacing pulse, it initially applies a positive voltage to stimulate the heart tissue. However, after the capacitive drop, this positive voltage (rising edge)is followed by a critical negative voltage phase, serving multiple purposes in the pacing cycle. This phase involves the voltage going negative before returning to zero, a process designed to counteract electrode polarization at the interface between the pacing electrode and the heart tissue. Electrode polarization, occurring after the positive voltage pulse, can interfere with the pacemaker's ability to sense the heart's intrinsic electrical activity and deliver effective pacing pulses. The reversal of this polarization is achieved through the negative voltage phase, which restores the electrode to a more neutral state. Additionally, this phase aids in maintaining charge balance around the electrode, ensuring no residual charge accumulates that might impact the heart tissue's response to future pacing pulses[14].

- **"Recharge Phase"**: Towards the end of the pulse in Figure B, there is a distinct phase where the voltage returns towards zero. This recharge phase is necessary to prepare the heart tissue for the next stimulus. During this phase, the pacemaker ensures that the electrode at the heart tissue is brought back to a neutral state, often via a reversal of the current flow, which helps prevent polarization of the electrode and ensures the tissue is ready for the subsequent pacing pulse.

  The recharge phase is critical because if the tissue remains polarized or charged, it might not respond appropriately to the next pacing pulse. This could lead to pacing inefficiencies or even failure to capture the heart rhythm, which is why modern pacemakers carefully control this phase to ensure reliable and consistent heart pacing .

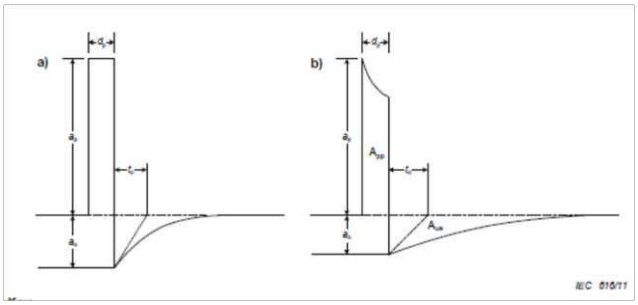

Figure 3.2: Pacemaker Impulse Profiles. a) Ideal PM Impulse: Standardized pulse with uniform amplitude and distinct onset and offset within a defined duration. b) Realistic PM Impulse: Capacitive drop at the onset, followed by a recharge phase ensuring tissue readiness for subsequent stimulation.

3.2.2 Stimulation impulse implemented by commercial pacemaker

In advancing the understanding of pacemaker functionality, it is paramount to assess how theoretical guidelines translate into actual clinical practice. Beyond the normative guidelines, the investigation extends to the actual parameters utilized in contemporary pacemakers. This critical evaluation ensure that the characteristics represented in the research database accurately reflect real-world PM settings. The characteristics of the database **'PacedECGDB'** will be explain in the next section. By scrutinizing the parameters of commercially available pacemakers, it was possible verifies that the range of pulse amplitudes, durations, and other electrical properties represented in the database encompasses the operational spectrums of these medical devices. It is a meticulous process that involves not only a comparison with the standards set by the International Electrotechnical Commission (IEC) but also an examination of the actual settings programmed in pacemakers during patient care.

In the forthcoming table (Table 3.1), a comparative analysis is presented, detailing the disparities and overlaps between the pacemaker pulse characteristics as defined by the normative guidelines, those observed in real-world pacemakers from industry leaders such as Biotronik and Medtronic[15][16], and the parameters encapsulated within the research database.

Table 3.1: Comparison of Pacemaker Pulse Parameters

	Medtronic	**Biotronik**	**IEC 60601-2-27**	**PacedECGDB**
Amplitude	From 0.25 to 6 V (0.25 step). From 6 to 8 V (step 1)	From 0.2 to 6 V (0.2 step). From 6 to 7.5 V (step 0.5)	(2-700) mV	(0.094 – 0.3) mV
Duration	(0.03 – 1.5) ms	(0.1 – 1.5) ms	(0.5 – 2)ms	(0.1 – 2) ms
Lower rate	(30,60...120) (min^{-1})	(30,60...120) (min^{-1})	100 (min^{-1})	100 (min^{-1})

The manufacturers' manuals was evaluated, providing the basis for understanding the range and scope of the operational parameters of these real pacemakers.

The first point of comparison is amplitude. Here, a marked contrast emerges: real pacemakers offer a wide amplitude range from 0.25 volts (V) up to 8 V, vastly exceeding the normative range of 2 to 700 millivolts (mV). This broad spectrum is reflective of the dual functionality of modern pacemakers, which, in addition to pacing, may also perform defibrillation, necessitating higher voltage outputs. The database adopts a narrower amplitude scope, ranging from 0.094 to 3 mV, with only the upper threshold falling within normative standards. This is a deliberate inclusion to accommodate the advancement in pacemaker technology where lower voltage spikes may be employed, a development that some modern devices incorporate. When examining pulse duration (PD), the ranges depicted by real devices, normatives, and the database exhibit considerable alignment. Real pacemakers display PDs stretching from 0.03 to 1.5 ms, which closely mirrors the normative guidelines spanning from 0.5 to 2 ms. The database's range is set from 0.1 to 2 ms, ensuring coverage of the entire spectrum seen in both real pacemakers and normative guidelines. Such consistency across all scenarios signifies the database's capacity to realistically simulate the pulse duration observed in clinical settings.

Similarly, the requirement for the rising edge duration remains constant across all three domains, with a uniform benchmark that it must be less than 0.1 ms. This parameter is critical, as it defines the sharpness and the promptness of the stimulus delivered to the heart tissue, a feature that must be precisely replicated in simulations to ensure the authenticity of the database.

Chapter 4

Elimination and identification algorithms for the removal of pacemaker stimulation patter from ECG traces

4.1 Databases used for algorithm validation

Pacemakers, small battery-operated devices, are essential in managing heart rhythm disorders by delivering electrical impulses to cardiac muscles, maintaining regular heart contractions and normal blood circulation. Their correct detection in ECGs is crucial for evaluating heart reactions, especially since modern pacemakers can generate smaller amplitude pulses that may be overlooked by standard detection algorithms. This issue is compounded by factors like electromyographic (EMG) noise, which can overlap with pacemaker frequencies, posing challenges in pulse detection [17].

The database used for testing detection and remotion algorithm is called **'PacedECGdb'**, the first publicly available database for ECGs with pacing pulses, vital for developing and testing pace detection algorithms in electrocardiography (ECG). It contains 1404 recordings, including 780 'pure' ECGs with pacing pulses and 624 paced ECGs corrupted by

tremor, offering a unique resource for researchers. HOwever, not all of these recordings are used. The database was designed to focus on ECGs that are pertinent to the application of pacemakers. This selection process involved:

- **Duration Limitation**: Each recorded ECG signal is limited to 10 seconds. This duration was deemed sufficient as the characteristics of the simulated ECG signals do not change significantly over time. Longer recordings would primarily increase the database size without adding substantial value.

- **Selection of specific ECG Leads**: ECG lead II was specifically chosen for mixing with pace pulses, as it displays the pacing pulses most effectively for a significant portion of paced patients.

- **Exclusion of Certain Programs**: From the HKP arrhythmia simulator's programs, only those generating sinus rhythm (SR) or arrhythmias compatible with pacemaker application were used. Special programs like long-term rhythm sequences, reanimation training, ventricular fibrillation, idioventricular rhythm, and bigeminy were excluded. The third-degree AV-block program was included to represent signals with this particular block.

- **Superimposing Pacing Pulses**: Pacing pulses corresponding to different pacemaker modes were superimposed over the selected ECG signals to create a comprehensive database that reflects a range of pacemaker types and modes. Moreover, the types of pacemaker superimposed to the traces is not always related or correspond to the arrhythmia.

The database aims to address the complexities of pacemaker pulse detection, providing a range of arrhythmias and pacemaker types for research, as shown in table 4.1.
It includes a variety of ECG rhythms generated by the HKP arrhythmia simulator, combined with pacing pulses that cover wide ranges of rising edge durations (from < 10 µs to 100 µs) and total pulse durations (from 100 µs to 2 ms). The amplitude of these pulses varies from twice the amplitude of normal heartbeats down to 100 µV, presenting a broad spectrum for testing detection methods .

Table 4.1: Correlation between HKP Program, Arrhythmia Type, and Simulated Pacemaker Type/Mode [17]

HKP Program	Arrhythmia Type	Pacemaker modality
P01	SR	Atrial pacing on demand
P02	SR + tremor	Fixed atrial rate pacing
P01 with tremor	AV rhythm	Ventricular pacing on demand
P02 with tremor	AV rhythm + tremor	Fixed ventricular rate pacing
P03	Atrial flutter combined with absolute arrhythmia	Ventricular pacing on demand
P03 with tremor	Atrial flutter combined with absolute arrhythmia + tremor	Fixed ventricular rate pacing
P06	SR with ventricular extrasystoles	Ventricular pacing before each normal beat (following sensed atrial activity)
P06 with tremor	SR with ventricular extrasystoles + tremor	Ventricular pacing before each normal beat
P08	SR with ventricular extrasystoles	Atrial pacing before each normal beat, on demand
P09	2nd degree AV-block	Fixed ventricular rate pacing (some of the pacing pulses are not effective)
P09 with tremor	2nd degree AV-block + tremor	Fixed ventricular rate pacing
P10	SR	Fixed pacing before each P-wave and QRS complex
P12	3rd degree AV-block with ventricular replacement rhythm	Bi-ventricular pacing
P12 with tremor	3rd degree AV-block with ventricular replacement rhythm + tremor	Bi-ventricular pacing
P13	SR with intermittent SA-block	Atrial pacing on demand + bi-ventricular pacing
P13 with tremor	SR with intermittent SA-block + tremor	Bi-ventricular pacing
P14	SR with bundle branch block	Fixed pacing before each P-wave and QRS complex
P14 with tremor	SR with bundle branch block + tremor	Fixed pacing before each P-wave and QRS complex

In the database, the amplitude of pacemaker (PM) pulses varies considerably, with a range extending from as low as 0.094 mV up to 3 mV. This variation is implemented through the use of a multiplication factor, Kp, which is associated with each ECG trace to determine the specific amplitude of its corresponding PM pulse. Six different Kp are applied to each traces, from the highest (Kp = 1 corresponds to 3mV amplitude), to the lowest (Kp = 0.03125 correspond to 0.094mV amplitude). Such a range of amplitudes, especially at the lower end, is noteworthy as it falls below the standard amplitude thresholds typically outlined in medical device norms and guidelines. However, it's crucial to note that pacemakers are designed to deliver a constant voltage to stimulate the myocardium effectively, and the current delivered is calculated based on the resistance in the lead tip, which is typically high to minimize battery depletion(18). The lowest amplitude in the range, 0.094 mV, has been deliberately excluded from the database. This decision is grounded firstly because amplitudes at this level represent an extreme scenario that is rarely, if ever, encountered in clinical settings. Pacemaker pulses are generally designed to be detectable and reliable, and as such, they typically exceed this minimal threshold. The settings of a

pacemaker, including its amplitude, are tailored to patient needs and optimized to ensure effective pacing and sensing. The sensing capability of pacemakers is designed to detect near-field depolarization currents, with thresholds set to ensure accurate detection and avoidance of irrelevant signals (18). Additionally, the relationship between the generated pacemaker pulses and the measurements at the body surface is a critical factor in pacemaker pulse detection. Understanding this relationship helps in setting specifications for pacemaker pulse detection among various device manufacturers. Studies show that there is a linear relationship between the programmed pacemaker amplitude and the amplitude recorded on the surface electrocardiogram, underscoring the importance of setting detectable and clinically relevant pacemaker pulse amplitudes.[19].

Additionally, pulses with such low amplitudes present significant challenges for accurate detection, often bordering on the limits of current technological capabilities. The risk of false negatives (i.e., failing to detect a pulse that is present) increases substantially at these levels, which could skew the results of algorithm testing and potentially lead to misleading conclusions about their efficacy.

Data collection was executed using the ADAS1000 evaluation board, which supports up to 10 ECG channels and includes an internal pace detection algorithm. This hardware setup provides a selection between different sampling rates and amplitude resolutions, with a high-resolution 128 kHz sampling rate to accurately capture the nuances of pacemaker pulses.

The ECG signals in 'PacedECGdb' are recorded with a 9.81 µV/LSB amplitude resolution at a 128 kHz sampling rate, ensuring detailed recording of pacing pulses. This high sampling rate is critical for capturing steep rising and trailing edges of pace pulses, and the signals can be down-sampled for research at lower rates [17].

Thirteen different pacing pulses were simulated in Matlab, as shown in the figures below (table 4.2), covering a variety of raising edge durations and pulse durations. The complexity of the pulses, involving multiple phases and varying durations, reflects the real-world variability in pacemaker technology.

Table 4.2: Characteristics of Pacing Pulses.

Pacing pulse	Rising edge duration (RE)		Pulse duration (PD)	
	No samples	Time	No samples	Time
PacePulse_01	2	7.8 μs	14	102 μs
PacePulse_02	3	15.6 μs	14	102 μs
PacePulse_03	4	23.4 μs	28	211 μs
PacePulse_04	5	31.3 μs	42	320 μs
PacePulse_05	6	39.1 μs	56	430 μs
PacePulse_06	7	46.9 μs	70	539 μs
PacePulse_07	8	54.7 μs	84	648 μs
PacePulse_08	9	62.5 μs	98	758 μs
PacePulse_09	10	70.3 μs	112	867 μs
PacePulse_10	11	78.1 μs	126	977 μs
PacePulse_11	12	85.9 μs	140	1086 μs
PacePulse_12	13	93.8 μs	210	1633 μs
PacePulse_13	14	102 μs	280	2180 μs

In the figure 4.1 the thirteen different pulses are represented.

Finally, the database includes a comprehensive annotation file, where each arrhythmia instance is meticulously documented with the onset of pacemaker (PM) pulses. These onsets are quantified in terms of the number of samples, as illustrated by the red dot in Figure 4.2. The placement of this red dot on the ECG trace corresponds directly to the annotated onset of the PM pulse in the number of samples, providing a visual reference for the associated annotation in the file. This annotation file serves a dual purpose. Firstly, it acts as a foundational reference for the validation of the detection algorithm, ensuring the accurate identification of PM pulses. Secondly, it forms the basis for the computation of statistical indices such as false positives (FP), false negatives (FN), and other relevant performance metrics. These indices are crucial for evaluating the efficacy of the detection algorithm and for refining its accuracy in identifying and analyzing cardiac arrhythmias.

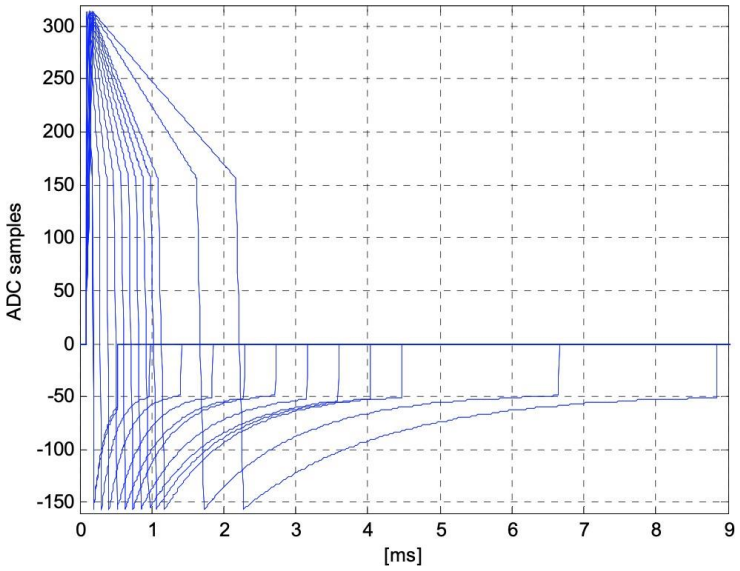

Figure 4.1: Visualization of the 13 pulses in time [17].

'Annotations'

704234
856653
1256519

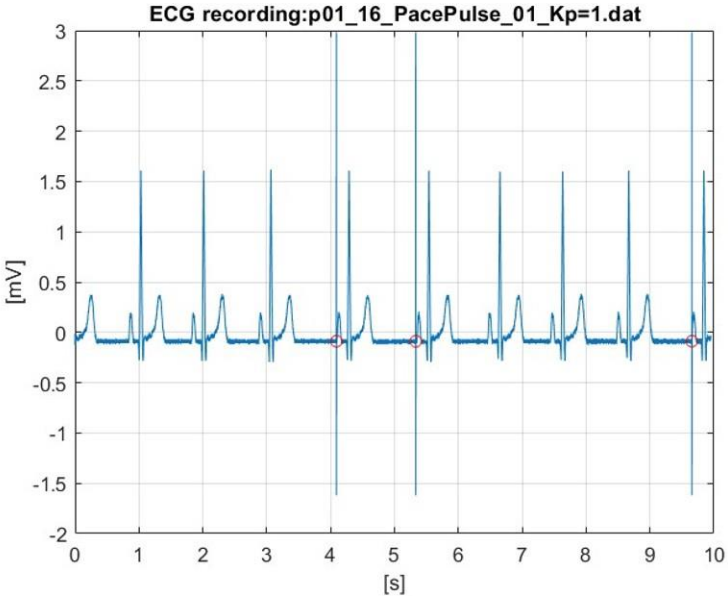

Figure 4.2: ECG trace generated in Matlab with related annotation corresponding to red dots.

4.2 Algorithms detection design

4.2.1 Mode algorithm

This section introduces the development and refinement of two distinct algorithms for pacemaker pulse detection and removal in ECG traces. Initially, algorithm adapted from existing literature was used , effective in pure scenarios but less so in noisy conditions. This limitation led to the creation of a more advanced algorithm, designed to accurately detect PM pulses irrespective of underlying noise. Here, their operational principles, modifications for enhanced accuracy, and the rationale behind transitioning from the initial approach to the final, more robust method, is highlighted.

The initial phase starts with an algorithm adapted from existing literature [19]. This algorithm operates on a principle of creating a window of N samples around each ECG sample, initially set to 3ms (1.5ms before and after each ECG sample), as shown in the scheme block represented in figure 4.3.

The crux of this method lies in calculating the difference between the reference point (the middle point of the window) and each point within the window. A PM peak is detected when this difference surpasses a predefined threshold. The threshold was established at 0.17 millivolt (mV) to ensure the identification of all PM peaks, which exhibit a wide amplitude range from 3 millivolt (mV) down to 0.1875 millivolt (mV). This particular threshold setting was strategically chosen to maximize the detection sensitivity for the majority of pulse amplitudes encountered (as explained before the lowest amplitude, 0.094, was excluded). By setting the threshold above this lowest value, the algorithm focuses on a more clinically relevant range of pulse amplitudes, enhancing its applicability and effectiveness. Once the peak is detected, the analysis was slitted of 10 millisecond (ms), ensuring that a single pulse was detected only one time.

The algorithm initially encountered challenges in accurately detecting pacemaker (PM) pulses, particularly when dealing with the lowest considered amplitude of 0.18 millivolt (mV). A significant issue was that, in some instances, the detection erroneously identified the PM pulse's trailing edge as the peak. This misidentification occurred because the reference point, or the middle of the window used for detection, occasionally fell along the

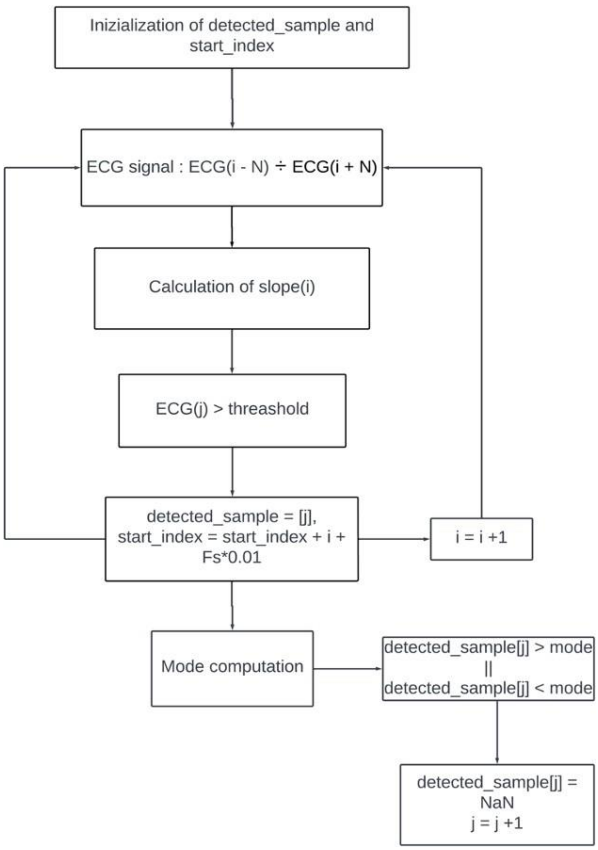

Figure 4.3: Scheme block of the first algorithm implemented.

rising edge of the PM pulse. Consequently, while computing the difference to detect the PM peak, the algorithm mistakenly picked up the opposite peak of the pulse(figure 4.4). To address this, a key adjustment was made in the window's duration, measured in milliseconds. This modification aimed to align the window more accurately with the rising edge of the PM pulse, known to comprise approximately 15 samples. A new function was implemented to calculate the difference between the actual start of the pulse (as marked in the database's annotation file) and the algorithmically detected peak position. If this difference exceeded 15 samples, it indicated an incorrect detection.

In the pursuit of optimizing the algorithm for pacemaker (PM) pulse detection, three distinct window durations were methodically evaluated: 2, 2.35 and 3 millisecond (ms). This experimentation was crucial in identifying the most effective window setting for accurate PM pulse detection across a variety of ECG traces. Remarkably, the 2.35 ms window emerged as the most proficient, striking a balance between sensitivity and specificity in

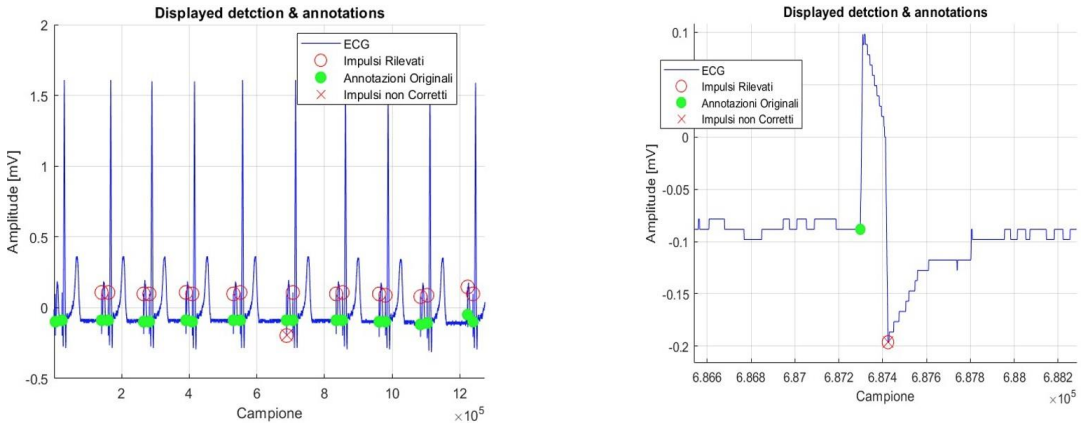

Figure 4.4: Accuracy problem founded for low PM amplitude. Detection occurs in the trailing edge as shown in the right figure.

pulse detection (see Chapter 6).

A further refinement of the algorithm was necessitated by specific challenges encountered in certain ECG trace types, such as those with a bundle branch block, where the QRS complex is characteristically wide (figure 4.5).

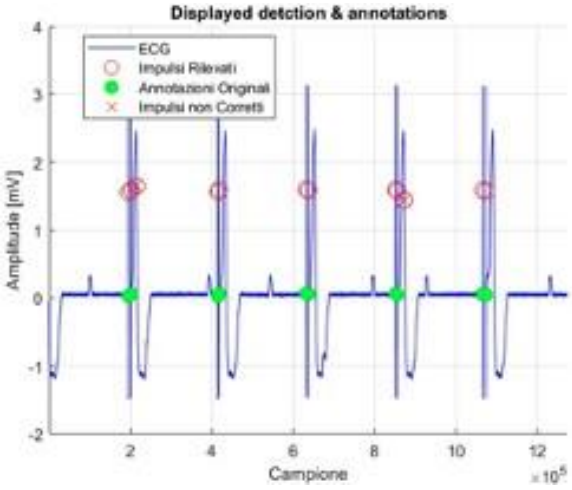

Figure 4.5: Bundle branch block showing a wide QRS complexes leading to detection of false positive (FP)

In these cases, even with adjusted window settings, the algorithm was prone to incorrectly identifying peaks within the QRS complex due to its distinct morphology, rather than accurately pinpointing the pacemaker (PM) pulses. Recognizing these limitations prompted the development of a custom enhancement to reduce false positives (FP). In pure cases,

where the baseline start of pulses is consistent, we implemented a secondary analysis involving the computation of the mode of the vector storing the peak values.

This approach aimed to discern genuine PM peaks from those falsely detected within the QRS complex. By analyzing the most frequently occurring values (the mode), the algorithm could effectively distinguish between the actual PM pulses and the morphologically induced false detections within the QRS complex. This innovative step allowed for the exclusion of peaks that deviated significantly from the mode, thereby refining our detection accuracy in noise-free scenarios.

Nevertheless, the real challenge surfaced when dealing with noisy ECG traces. The original algorithm's reliance on baseline initiation of PM pulses became the biggest limit in the face of EMG noise. This issue is exemplified in figure 4.6 , where the algorithm's performance in noisy conditions is illustrated.

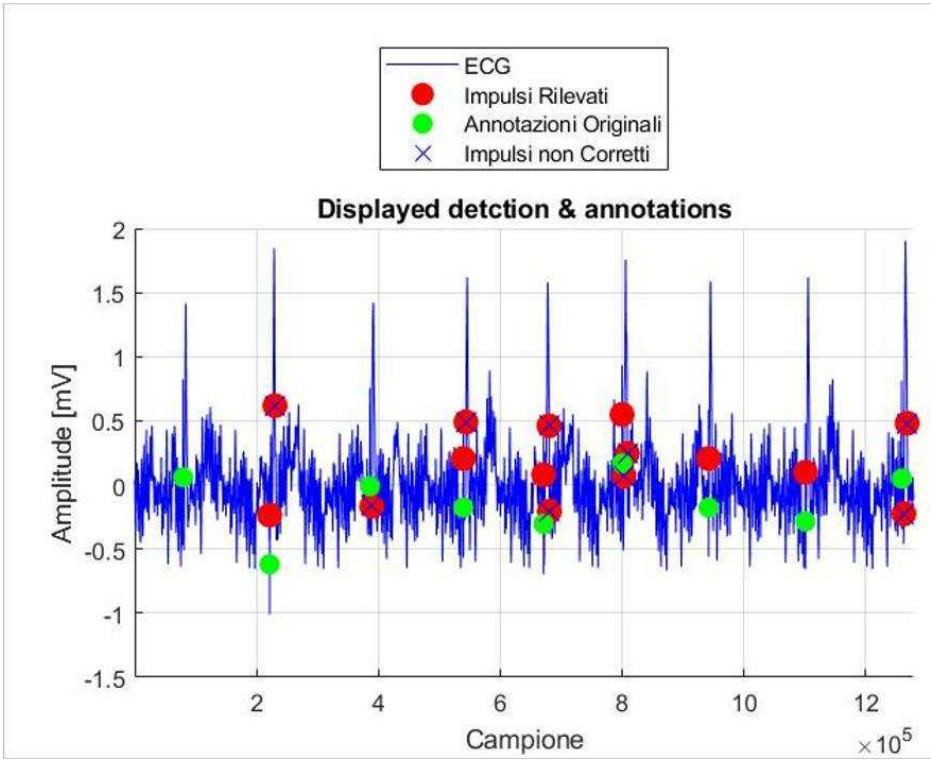

Figure 4.6: Noisy traces (EMG noise), leading to improper detection and many false positives (FP)

4.2.2 Rising edge based algorithm

This necessity led to the development of an advanced algorithm, designed to effectively manage the complexities introduced by noisy ECG environments, as demonstrated in Figure 4.6. This figure represents the incorrect detections made by the previous algorithm when faced with noisy ECG traces. The inaccuracy arises due to the computation of the mode being meaningless in these scenarios. As illustrated by Figure 4.6, the impulses (green dot), distorted by muscle contraction noise superimposed on the trace, initiate from different positions, with some starting from positive values and others from negative ones. This variability results in the algorithm's inability to consistently determine the correct onset of the pacemaker pulse, highlighting the need for a more robust solution.

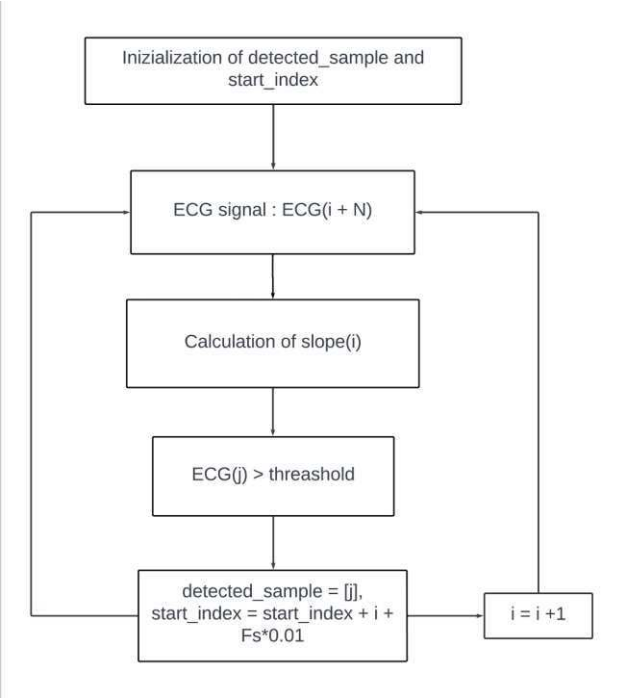

Figure 4.7: Scheme block of the final algorithm.

Given these challenges, it became clear that a new direction was needed. Consequently, a more straightforward approach was devised for the second algorithm. This new method was developed to address the shortcomings observed in the first algorithm, particularly to enhance detection accuracy in the context of noisy ECG traces. By simplifying the detection mechanism, the second algorithm aims to provide a more reliable identification

of pacemaker pulses, even amidst the variability presented by muscle contractions and other forms of noise.This algorithm capitalizes on a critical feature of PM pulses – their rising edge. Given that the ECG data is sampled at 128 kiloheartz (kHz), and in accordance with normative guidelines stating that the rising edge of a PM pulse is less than 100 microseconds, the rising edge is estimated to encompass approximately 15 samples. This insight led to a novel method of PM pulse detection. Rather than examining a window of samples before and after each ECG sample, the algorithm considers a window of 15 samples following each ECG sample, as shown in figure 4.7. If the difference between the ECG sample and any value within this window exceeds a predefined threshold (0.17 millivolt (mV)), a PM peak is identified. This method is particularly effective in noisy conditions, as it primarily focuses on the steep, distinguishable feature of the PM pulse – its rising edge – thereby ensuring accurate detection. This second algorithm represents a significant simplification in approach, yet it provides a robust solution to the challenges posed by noisy ECG data. Its effectiveness lies in its ability to directly target the most distinctive aspect of the PM pulse, thereby reducing the likelihood of false positives or negatives that were more prevalent in the first algorithm.

In advancing the algorithm's capabilities, a crucial development was its effectiveness in both pure and noisy ECG trace conditions. After excluding certain traces, such as those with the lowest amplitude that were deemed clinically irrelevant, the total number of ECG traces considered for comprehensive testing was 936. This refined set of traces ensures that the algorithm's performance is assessed on data representative of typical clinical scenarios, enhancing the robustness and reliability of the results

4.3 Algorithms removal design

Having successfully developed an algorithm for PM pulse detection, the next critical step towards refining ECG analysis is the design of an algorithm for PM pulse removal. This phase seeks to address the challenge posed by PM pulses by eliminating them from ECG traces, allowing for a cleaner and more accurate representation of the patient's intrinsic

cardiac activity.

In exploring the literature on pacemaker pulse removal in ECG analysis, a variety of methods were identified. One such method [20] involves a novel framework using autoregression, weighted mean, and linear interpolation, focusing on minimal intervention and efficient artifact removal. Despite these diverse approaches found in the literature, the project specifically implemented two distinct algorithms: the ”Flattening method” and the ”Interpolation Method.” These chosen methods, while sharing fundamental principles with those found in existing research, were uniquely adapted to address the challenges of PM pulse interference in ECG traces. By focusing on these two algorithms, the project aimed to enhance ECG data quality and accurately represent the patient’s intrinsic cardiac activity, ultimately improving ECG analysis in the presence of pacemaker pulses.

In the pursuit of refining the analysis of Electrocardiography (ECG) signals, particularly in the presence of Pacemaker (PM) pulses, two algorithm was developed for the removal of PM, based on the two methods mention before. These methods, although not following the exact block scheme found in existing literature, are underpinned by the same fundamental approach and principles.

The first method, **”Flattening method”**, involves identifying the presence of PM pulses within ECG traces and subsequently defining a window around the PM pulse that is then flattened. This transformation is underpinned by the premise that the PM pulse, although initially obtrusive, can be segregated and isolated without losing vital information about the patient’s cardiac rhythm, even if the ECG morphology in correspondence of the pulse is distorted, reducing the PM pulse to a well-defined segment. In the second method, **”Interpolation Method”**, we take a different yet complementary approach to PM pulse removal. Here, the primary objective is not just to eliminate PM pulses but also to enhance the representation of the ECG morphology in the regions affected by the PM pulse. This method leverages interpolation techniques to reconstruct the ECG signal in areas where PM pulses were detected. By intelligently interpolating data points, the aim was to recreate the underlying cardiac activity with greater fidelity, ensuring that the ECG traces reflect the patient’s actual cardiac rhythm more accurately. In both methods, the overarching goal is to enhance the quality of ECG data by minimizing the interference

caused by PM pulses. The removal algorithms for pacemaker (PM) pulses in both cases were designed with careful consideration of two key characteristics of the PM pulse: the duration of its rising edge and its total duration. The algorithms specifically target these aspects to accurately isolate and remove the PM pulse from the ECG trace.

- **Rising Edge Duration**: The detection of the PM pulse consistently occurs on the rising edge, a crucial feature of the pulse. According to the parameters set by relevant medical standards, this rising edge has a maximum duration of 100 microseconds, which corresponds to approximately 15 samples at a sampling rate of 128 kHz. Therefore, in both removal algorithms, the number of samples considered for the removal process, starting from the point of detection, is calibrated to cover a duration of 0.2 milliseconds. This duration is chosen to ensure that the entire rising edge of the pulse is encompassed.
- **Total Pulse Duration**: The other significant characteristic considered is the total duration of the PM pulse. Given that the longest duration a PM pulse can have is approximately 9 milliseconds, the algorithms are designed to extend the window of removal to 10 milliseconds to the right of the detection point. This ensures that the entire PM pulse, regardless of its specific duration within the possible range, is captured and removed from the ECG trace.

By aligning the window dimensions with the rising edge and total duration of the PM pulse, the algorithms achieve a precise and comprehensive removal of the pulse, effectively isolating it from the rest of the ECG trace. This methodical approach is essential for maintaining the integrity of the remaining ECG data, ensuring that only the PM pulse is removed while preserving the crucial cardiac information contained in the ECG.
The window created for all the PM pulses detected are show below (1).

$$\mathbf{ECG}(j - N) \div \mathbf{ECG}(j + K) \tag{1}$$

where:

- j represents the sample where the PM pulse is detected
- N is equal to 0.2 millisecond (ms)
- K is equal to 10 millisecond (ms)

Am image of the window create around the pulse is shown in figure 4.8.

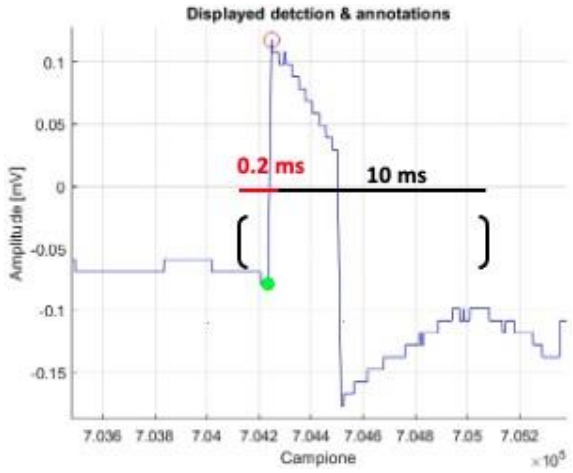

Figure 4.8: Window removed from each PM pulse detected

4.3.1 Flattened method

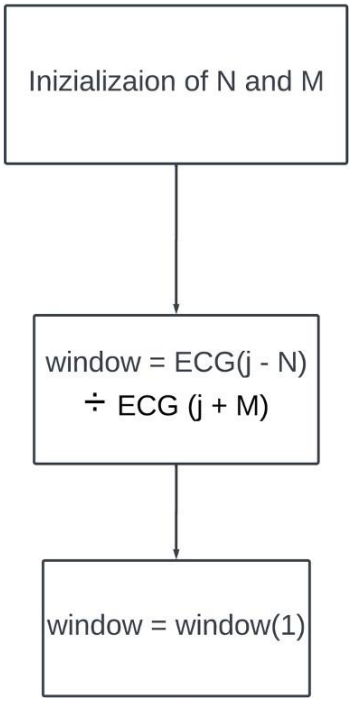

Figure 4.9: Scheme block of the remotion algorithm using flattening method

In the scheme block presented above, we detail the procedure for removing the pacemaker (PM) pulse using the 'Flattened Method.' This method is a straightforward approach for PM pulse removal in ECG traces, focusing on simplicity and efficiency [20].

Once the PM pulse is detected within an ECG trace, the algorithm initiates a window as previously defined – a span that covers the rising edge and the total duration of the PM pulse. The window is critical in isolating the PM pulse for removal. In the Flattened Method, once this window is established, the algorithm proceeds to replace the entire PM pulse with a flat segment. This is achieved by assigning the first value of the window to all samples within it. Essentially, the segment of the ECG trace where the PM pulse is located is flattened to a constant value, effectively 'erasing' the pulse from the waveform (figure 4.10).

However, it's important to note that while this method is effective in removing the PM pulse, it does not preserve the natural morphology of the ECG in the affected region. The result is a segment of the ECG that, though free from the PM pulse, lacks the physiologi-

cal waveform typically seen in an uninterrupted ECG trace.

To address this limitation and achieve a morphology that more closely resembles a natural ECG waveform, an interpolation-based method was subsequently implemented. This advanced approach not only removes the PM pulse but also interpolates the surrounding ECG data to reconstruct the waveform in the pulse's place. The interpolation method provides a more aesthetically and clinically accurate ECG trace, particularly in the segments where the PM pulse has been removed.

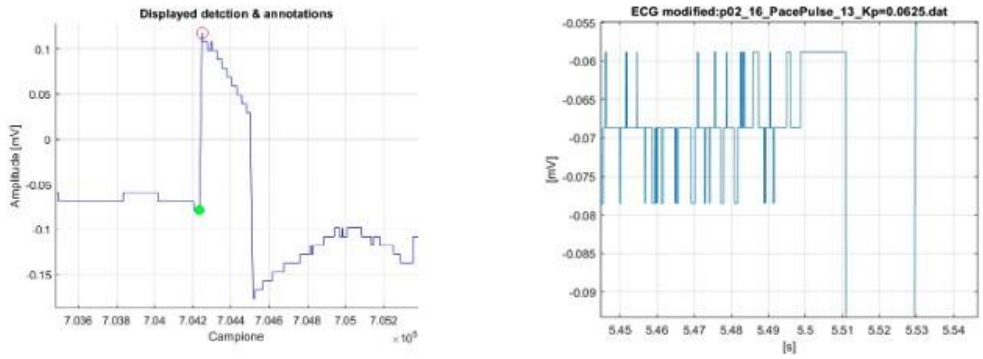

Figure 4.10: Visualization of the PM pulse replaced by a segment

4.3.2 interpolation method

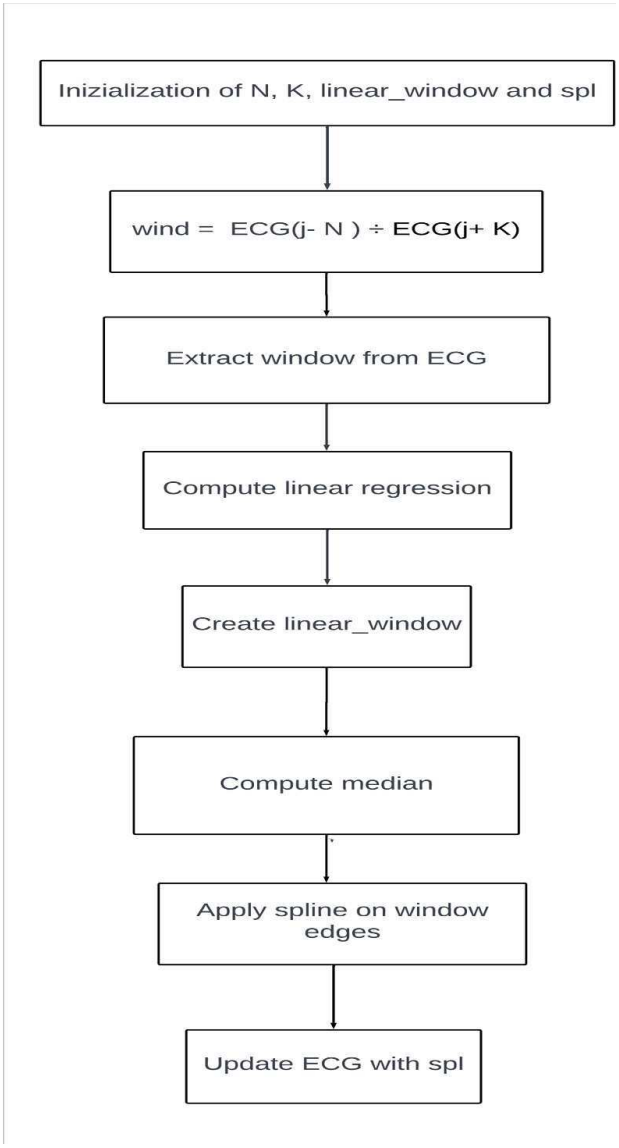

Figure 4.11: Scheme block of the remotion algorithm using interpolation method

In the scheme block presented shown in figure 4.11, the 'Interpolation Method' is represented for pacemaker (PM) pulse removal in ECG traces. This method, drawn from existing literature [21], involves an initial approximation of the PM pulse using a linear regression function. The approach replaces the PM pulse with a straight line that connects the highest and lowest points of the pulse, effectively creating an initial approximation that serves as a basis for further refinement (figure 4.12).

Building upon this literature-based approach, a novel implementation has been added to

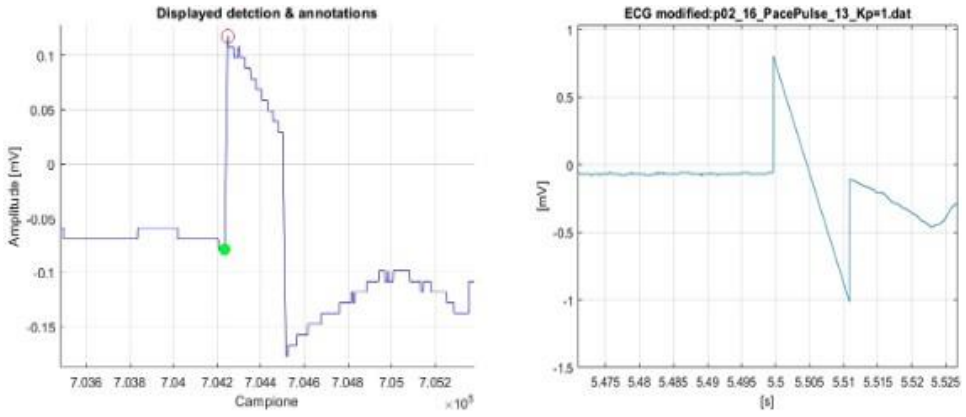

Figure 4.12: Initial approximation of the pulse using linear regression

enhance the interpolation process. Instead of relying solely on the linear regression line, the median of this line is calculated to establish an intermediate point. This step is crucial for the subsequent spline interpolation, as it provides a more representative point that reflects the general trend of the ECG data within the window.

The spline function, a smooth and flexible interpolation tool, is then employed to create a more physiologically accurate waveform. Within the predefined window that encompasses the PM pulse, the spline function connects the first and last points of the window with the median point of the linear regression line. This method ensures a smooth transition between the natural ECG data and the interpolated segment, preserving the waveform's continuity, as shown in the figure 4.13.

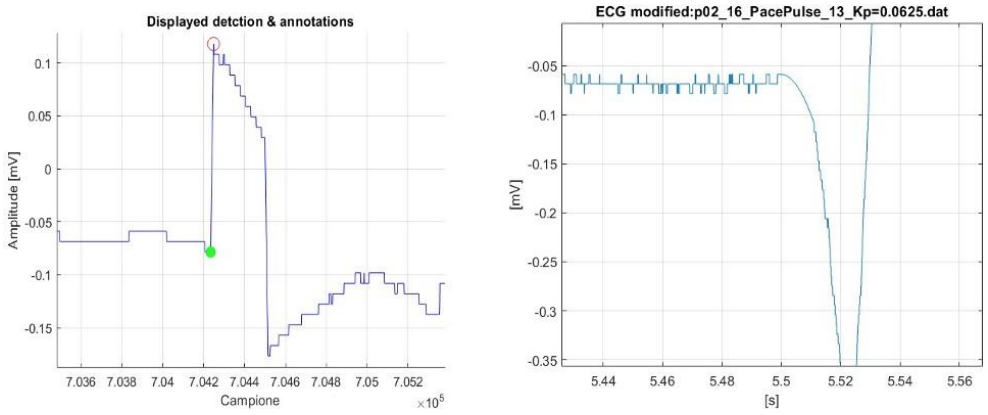

Figure 4.13: Pacemaker pulse replacement with Spline Interpolation

The process culminates with the replacement of the original PM pulse within the pre-defined window using the spline function. This window, as established at the beginning of the process, encompasses the entire PM pulse, taking into account its duration and the characteristic rising and falling edges. The spline function, which now includes the first point of the window, the median of the linear regression line, and the last point of the window, is applied to this specific segment of the ECG trace.

By replacing the original PM pulse with the output of the spline function, the algorithm achieves a seamless integration of the interpolated segment into the overall ECG waveform. This replacement is done in such a way that the continuity and the natural pattern of the ECG are maintained. The spline function's ability to create a smooth, natural-looking curve ensures that the reconstructed segment does not appear artificially inserted or out of place, thus preserving the waveform's physiological relevance.

In essence, the Interpolation Method, with its final step of replacing the PM pulse using the spline function, offers a sophisticated solution to PM pulse removal. It addresses the need for accurate pulse elimination while ensuring that the resulting ECG trace remains a faithful representation of the cardiac activity, free from the distortions introduced by the presence of the PM pulse. This approach exemplifies the blend of precision and practicality, essential in the field of biomedical signal processing, particularly in applications involving complex physiological signals such as ECGs. The rationale for using the median of the linear regression line as an intermediate point for the spline is rooted in the typical morphology of the PM pulse. PM pulses generally have both positive and negative components, creating a distinct peak-and-trough pattern. By connecting the highest and lowest points of the pulse and then taking the median, we effectively capture a central point that lies within the natural progression of the ECG waveform. This point serves as an ideal anchor for the spline interpolation, ensuring that the reconstructed waveform closely mimics the natural shape and trend of the ECG data.

Chapter 5

Algorithm validation

The validation phase of the project was designed as a rigorous testbed to evaluate the effectiveness of the developed pacemaker (PM) pulse removal algorithms. This phase was integral in assessing how well the algorithms integrated with the company's existing arrhythmia detection software. Given the software's limitation in accurately detecting arrhythmias in the presence of PM pulses, our primary objective was to ensure that the removal of these pulses enhanced the software's performance.

The approach began by selecting ECG traces from our comprehensive database. These traces, each with its unique arrhythmic characteristics, were processed through our PM pulse removal algorithms. Once the pulses were effectively removed, the modified ECG traces were ready to be analyzed by the company's software. However, introducing these traces into the software ecosystem required several critical steps.

One of the pivotal elements of our validation setup was the Prosim8 device. This device provided a variety of arrhythmia simulations, which were essential for a comparative analysis. By connecting the company's arrhythmia detection hardware to Prosim8, we could juxtapose the arrhythmias from our database against the simulations. This comparison aimed to validate the consistency and reliability of the arrhythmia detection post-PM removal. It was crucial to determine if the removal algorithms distorted the ECG's inherent arrhythmic properties or if they maintained the trace's integrity for accurate analysis.

The display and analysis of results were facilitated by the WinMultiServer software. This software, connected wirelessly to the company's hardware, played a vital role in visually

presenting the outcomes of the arrhythmia detection process. The ability to monitor these results in real-time was invaluable, offering immediate insights into the algorithms' performance and the software's arrhythmia detection capabilities.

A significant technical consideration in our validation process was the format and handling of the ECG data. The WinMultiServer software necessitated the ECG traces in a specific .txt format, a requirement that led to the transformation of our database traces into a compatible format. This conversion process involved meticulously formatting the data to include the number of samples, the sampling frequency, ECG derivation details, and the trace values in millivolts.

Furthermore, adapting to the technical constraints of the company's software was essential. The original high sampling rate of 128 kHz from our database traces exceeded the software's capacity. To resolve this, we implemented a downsampling process, reducing the sampling rate to 4 kHz, aligning with the software's maximum threshold. This step was not just about ensuring technical compatibility; it was also about preserving the fidelity of the ECG data to the greatest extent possible, despite the reduced sampling rate.

The detailed procedure encompassing the integration of our algorithms with the company's arrhythmia detection software and the subsequent analysis is illustrated in the figure below (figure 5.1). This visual representation provides a clear and concise overview of the entire validation process, from the initial data handling and algorithm application to the final analysis and display of results.

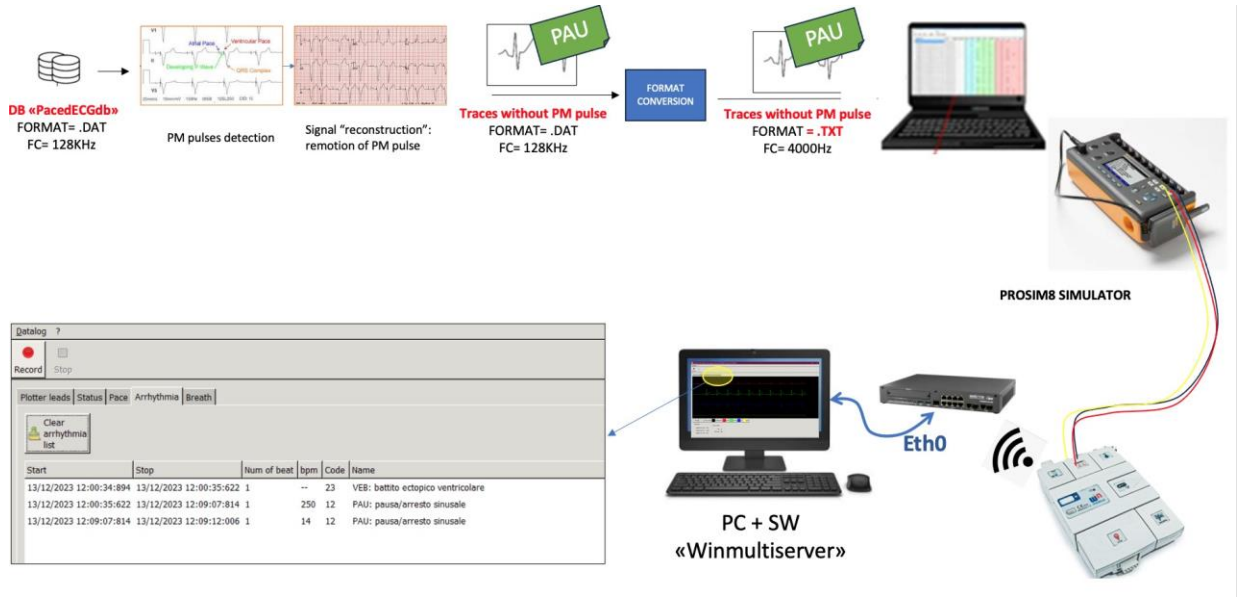

Figure 5.1: Procedure followed to validate algorithms implemented

In the project, a pivotal aspect of evaluating the effectiveness of the algorithms was understanding the operational nature of the company's arrhythmia detection software. The software does not directly identify arrhythmias per se but rather detects abnormalities that are typically associated with various arrhythmias (figure 5.2).

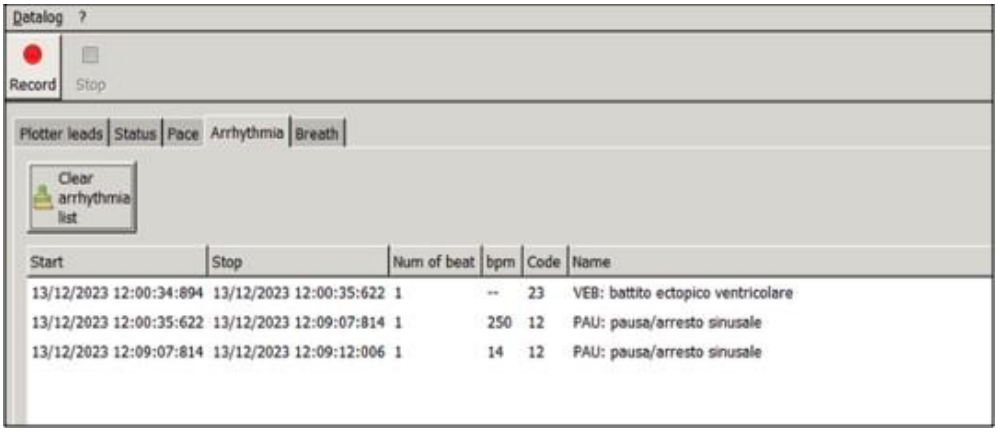

Figure 5.2: Visualization of the output generated by the software. Detection of abnormalities related to the corresponding arrhthmia

This nuanced approach to arrhythmia detection necessitated a thorough understanding of the correlation between specific arrhythmias and their related abnormalities as identified by the software. Such an understanding was crucial to accurately assess whether our algorithms were effective in facilitating the correct identification of arrhythmias post-PM pulse removal. To illustrate, let's consider the types of arrhythmias present in our database and the corresponding abnormalities that the software was likely to identify:

- **Sinus Rhythm**: This is the normal heart rhythm, typically characterized by an upright P wave in lead II and a biphasic P wave in V1. The software would usually not report any abnormalities in this rhythm, as it represents the standard rhythmic function of the heart.

- **Atrial Flutter**: This arrhythmia is characterized by a fast and regular cardiac rhythm, often seen on ECG as a "saw-tooth" appearance of P waves with a variable degree of AV block. The software might identify this as Supraventricular Ectopic Beats (SVEB), a consistent finding for this type of arrhythmia.

- **Ventricular Extrasystole**: Identified by an extra beat originating from the ventricle, it typically results in a wide QRS complex on ECG due to slow conduction through the ventricles. The software would classify it as Ventricular Ectopic Beats (VEB). PVCs, like ventricular extrasystole, are common and can occur in both healthy and unhealthy individuals.

- **2nd Degree AV Block**: Typically associated with a prolonged PR interval, this block can present with dropped beats. In our dataset, it's characterized by the absence of QRS complexes, leading to the software detecting a pause. AV blocks involve delayed or blocked conduction of impulses from the atria to the ventricles.

- **3rd Degree AV Block**: Involves a complete dissociation between the atria and ventricles, indicated by prolonged PR intervals and enlarged QRS complexes. The software would likely detect this as a proper pause. This block represents a severe form of heart block where the atria and ventricles beat independently.

- **Bundle Branch Block**: Marked by an enlarged QRS complex, it indicates a delay or block in the conduction pathway within the ventricles. In our dataset, it's a simplified situation where the detection of VEB is not generally associated with actual VEBs.

- **SA Block**: Characterized by pauses and sinus arrests, this block occurs when the electrical impulse from the SA node is not properly transmitted. It can lead to a slow heart rate and can be asymptomatic or cause symptoms like dizziness or syncope. The software might identify this as a pause or a delay.

The detailed characteristics of these arrhythmias are key indicators used in clinical practice for diagnosis. Similarly, recognizing the significance of prolonged PR intervals and the patterns of conduction block in different types of AV Blocks can inform appropriate medical interventions. The specific ECG findings associated with these arrhythmias provide valuable insights into the underlying cardiac conditions, aiding clinicians in delivering targeted and effective treatment [24][25].

Understanding these correlations was essential for our validation process. By comparing the output from the software against the known arrhythmia types from our database, we could determine if our algorithms for PM pulse removal were effective in preserving the ECG's diagnostic integrity. This comparative analysis required meticulous attention to the software's interpretation of ECG abnormalities, ensuring that the removal of PM pulses did not inadvertently alter the fundamental arrhythmic characteristics of the ECG traces.

Chapter 6

Results evaluation

6.1 Detection and removal algorithms

In this section, we will dissect the performance of each algorithm. The evaluation is based on a series of metrics designed to test their accuracy, reliability, and robustness in both pure and noisy ECG trace conditions. By carefully examining the results obtained from applying these algorithms, we gain valuable insights into their capabilities and limitations.
The evaluation of the first algorithm developed for pacemaker (PM) pulse detection, was particularly significant, firstly, as it reveals the efficacy of the initial algorithm under various test conditions, and how the optimization of window duration played a pivotal role in its performance, secondarily, because its performance in the presence of noise revealed critical limitations that were instrumental in guiding the development of the second algorithm.
Recall from the algorithm development phase, we undertook a detailed examination of three specific window durations – 2 ms, 2.35 ms, and 3 ms – to ascertain the most effective setting for capturing PM pulses.
The effectiveness of the 2.35 ms window was underscored by its performance in a comprehensive analysis of 650 pure traces. In this evaluation, it exhibited a high degree of accuracy, with only four instances of false negatives (FN) identified (table 6.1).
The selection of the 2.35 ms window, which emerged as the most proficient in striking a balance between sensitivity and specificity, was a critical decision that significantly impacts the results we are about to delve into.

Table 6.1: Your table caption

Window size	**2 ms**	**3 ms**	**2.35 ms**
Algorithm works for	p01, p02, p03, p06, p08, p09, p13 (every PD and amplitude)	p01, p02, p03, p06, p09, p13	p01, p02, p03, p06, p08, p09, p10, p13
Algorithm does not work for	p10, p12, p14	p08, p10, p12, p14	p12, p14
Particular cases where algorithm does not work	**P10 (sinus rhythm)** PP01_0.125 - PP03_0.25 - PP07_05 - PP08_05 **P12 (3rd AV block)** PP12_0.0625 - PP12_0.0625 - PP12_0.0625 - PP12_0.0625 **P14 (bundle branch block)** PP12_0.0625 - PP13_0.0625	PP08_PP02_1 Several cases for p12, p14	**P12 (3rd AV block)** PP03_1 **P14 (bundle branch block)** PP08_05 – PP12_0.0625 - PP13_0.0625
Total cases	650 performed: **639 works 11 fails (FP)**	Greater than 200 performed: Works for the simpler arrhythmias but does not work in several case for p12 and p14.	650 performed: **646 works 4 fails (FN)**

Table 6.1 shows the results of these window setting in the detection of the pulse. In particular:

- **2 ms Window**: The algorithm, when set to a 2 ms window duration, demonstrated commendable performance overall. However, it identified 11 false positives (FP) across three types of arrhythmias: sinus rhythm, 3rd degree AV block, and Bundle Branch Block (BBB). A plausible explanation for the FPs, especially in the cases of 3rd degree AV block and BBB, is likely related to the challenges posed by the lowest amplitude pulses. In these instances, the shorter window duration may not have been sufficient to accurately differentiate between the PM pulses and the complex waveform patterns inherent in these particular arrhythmias. The lower amplitude

pulses, blending more seamlessly with the ECG's baseline, could have led to misinterpretations by the algorithm.

- **3 ms Window**: For the 3 ms window setting, the algorithm's effectiveness varied significantly. Notably, in more complex arrhythmias such as Bundle Branch Block, the algorithm did not perform consistently across all traces. In fact, more than 200 traces in such complex arrhythmias were inadequately processed. This inconsistency could be attributed to the longer window duration failing to precisely isolate the PM pulses within the intricate waveforms of these arrhythmias, leading to a higher likelihood of erroneous pulse detection.

- **2.35 ms Window**: The most promising results were observed with the 2.35 ms window duration. In this setting, the algorithm exhibited a marked improvement, with only 4 false negatives (FN) being detected. These FNs were primarily associated with the 3rd degree AV block and Bundle Branch Block arrhythmias. The better performance in this window setting can be attributed to its ability to balance the need for encompassing the PM pulse entirely without excessively overlapping with the natural ECG waveform, particularly in arrhythmias with complex morphology.

This result was particularly noteworthy given the complexity and variability inherent in ECG trace data. It's important to note that these results were obtained through manual analysis rather than automated statistical indices. This approach was chosen due to the algorithm's limitations in handling traces with tremor noise, where conventional statistical measures might not accurately reflect its performance. Consequently, the statistical analysis and computation of indices were reserved for the final algorithm, which was designed to address the broader challenges, including those presented by tremor-affected traces.

The second algorithm is a response to the need for an effective tool capable of handling the complexities introduced by EMG noise in ECG traces, underscored by the limitations revealed when applying the first algorithm to ECG traces affected by tremor, as illustrated in the previous figure (Figure 4.1). In this section, we revisit the same traces showcased in Figure 4.1, now highlighting the correct detection capabilities of the final algorithm (figure 6.1). This direct comparison between figures underscores the enhancements and accuracy

improvements realized in the development of the second algorithm, offering a clear visual representation of its efficacy in overcoming the specific challenges of EMG noise.

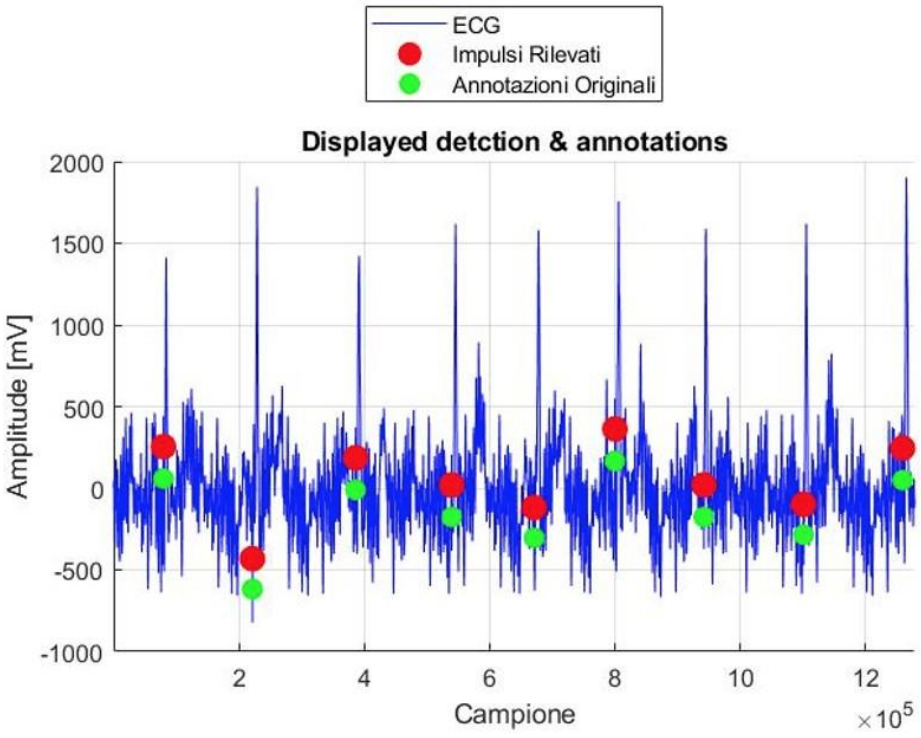

Figure 6.1: Detection using the first algorithm for traces with superimposed muscle contraction

An important aspect of this algorithm is its non-reliance on pre-filtering the ECG trace. Filtering, a common step in signal processing, could potentially alter or diminish the characteristics of the PM pulse, particularly its defining rising edge. By avoiding this, the algorithm preserves the integrity of the original ECG signal, ensuring that the crucial features of the PM pulse remain intact for detection. An additional facet of this research involved experimenting with various sampling frequencies. While the algorithm was initially designed for a high sampling rate of 128 kHz, not all ECG recording devices operate at such frequencies. Therefore, it was imperative to test the algorithm's performance at lower sampling rates to gauge its utility in more typical clinical settings.

To quantitatively assess the algorithm's performance, key statistical indices were computed for each frequencies tested and then compared: sensitivity, specificity, and Positive

Predictive Value (PPV). These metrics provide a robust framework for evaluating the algorithm's accuracy and reliability in detecting PM pulses.

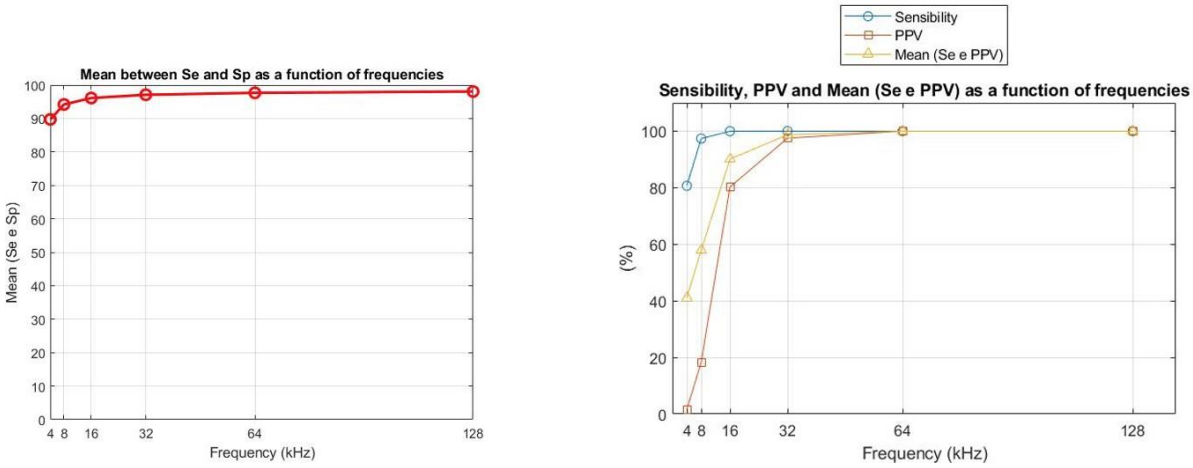

Figure 6.2: Comparison among different frequency. The left figure shows the mean between specificity and sensitivity. The right one shows the sensitivity, PPV, and the mean between them.

Table 6.2: Percentage values for sensitivity and positive predictive value

Frequency (kHz)	128	64	32	16	8	4
Se (%)	100	100	100	99.97	97.37	80.66
PPV (%)	100.00	100.00	97.50	80.25	18.29	1.56

The results are shown in figure 6.2 with the percentage values for sensitivity and positive predictive values reported in the table 6.2. The results from the pacemaker pulse detection algorithm show exceptional performance at higher frequencies, particularly at 128 kHz and 64 kHz, where the sensitivity (Se) and positive predictive value (PPV) both achieved perfect scores of 100%. This indicates that at these higher sampling rates, the algorithm is extremely effective in identifying and handling pacemaker pulses without false detections. However, there is a slight decrease in PPV at 32 kHz, hinting at an increase in false positives, which underscores the need for a balance between high accuracy and manageable false detections as the frequency decreases. At significantly lower frequencies, specifically 4 kHz and 8 kHz, revealed a marked decrease in accuracy. This inaccuracy can be attributed to the distortion of the PM pulse at these reduced sampling rates. Given that a PM pulse

is a rapid event, typically occurring within a 2ms window, a higher sampling frequency is crucial to capture its distinct characteristics accurately. At lower frequencies like 4 kHz and 8 kHz, the finer details of the PM pulse are lost, leading to its distortion and consequently, a decline in the algorithm's ability to reliably detect these pulses (figure 6.3).

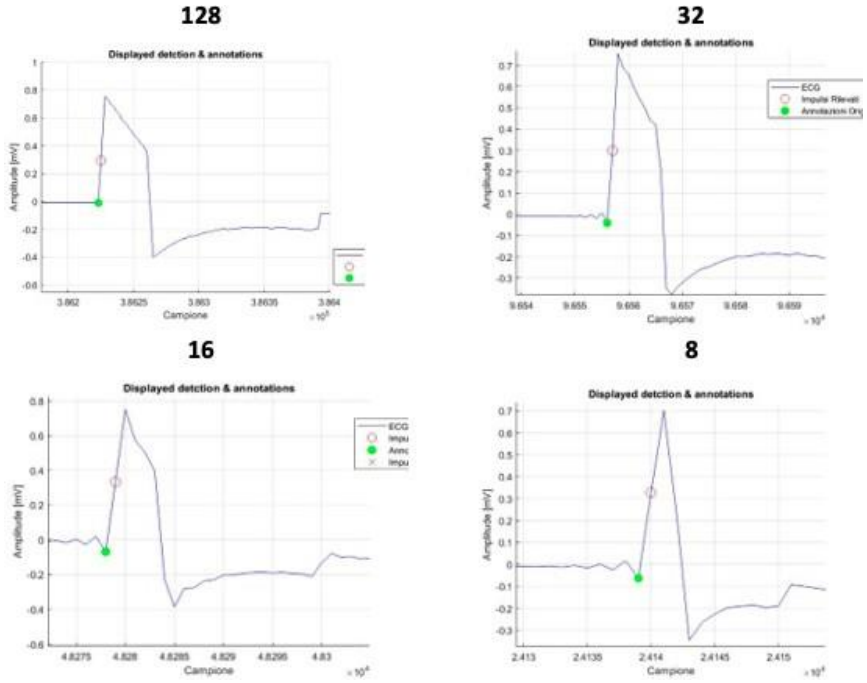

Figure 6.3: Comparison of PM Pulse Detection at Various Sampling Frequencies.

This observation underscores the importance of a sufficiently high sampling rate in the effective detection of PM pulses. While it's advantageous to develop an algorithm that performs well across a range of sampling frequencies for broader applicability, there is a critical threshold below which the fidelity of the ECG signal, and hence the accuracy of PM pulse detection, is compromised. This finding highlights a key consideration in the design and implementation of pacemaker detection algorithms, especially in the context of varying capabilities of ECG recording equipment.

In summary, while the algorithm demonstrated robust performance at high sampling rates, its efficacy diminished at lower frequencies, emphasizing the need for a balance between algorithm adaptability and the technical limitations of ECG recording devices. These insights not only inform the practical deployment of the algorithm but also contribute to the broader understanding of the technical requirements for effective pacemaker pulse

detection in diverse clinical settings.

6.2 Validation results

The validation process involved a comprehensive comparison between the ECG traces from the database, processed through the algorithms, and the arrhythmia simulations provided by the Prosim8 device. The objective was to assess the consistency and accuracy of the arrhythmia detection by the company's software post-PM pulse removal. Among various arrhythmias analyzed, the results for Sinus Rhythm, Atrial Flutter and SVEB Detection, Ventricular Extrasystole and VEB Detection, and Sinoatrial Block and Pause Detection stand out as the most reliable. This reliability is attributed to the high degree of similarity in morphology between these specific arrhythmias in the PacedECGDb and their counterparts in the Prosim8 simulations. Such morphological consistency is crucial for ensuring that the algorithms accurately detect and classify arrhythmias, as it minimizes the potential for discrepancies that could arise from differences in the presentation of the same arrhythmia across different sources. The results, displayed and analyzed via the WinMultiServer software, provided a clear visual representation of the algorithms' performance. This stage of the research is crucial in determining the real-world utility of the algorithms, particularly in the context of integrating them with existing clinical software for arrhythmia detection. The high morphological similarity in the arrhythmias discussed ensures that our validation process is grounded in a realistic comparison, highlighting the algorithms' effectiveness in scenarios where morphology between simulated and real ECG traces closely aligns.

The results obtained from the validation of the algorithms provide significant insights into their effectiveness in enhancing arrhythmia detection when integrated with the company's software. These outcomes are particularly revealing in cases where pacemaker (PM) pulses are present in ECG traces.

- **Sinus Rhythm** : In instances of sinus rhythm, where no arrhythmia is inherently present, the company's software erroneously detected abnormalities when PM pulses were included in the traces. However, when these PM pulses were removed using the developed algorithms, the software correctly identified the traces as normal, devoid of any arrhythmias. This stark contrast underscores the algorithms' effectiveness

in eliminating false abnormalities induced by PM pulses, thereby ensuring accurate detection of true sinus rhythm (figure 6.5).

- **Atrial Flutter and SVEB Detection**: For traces simulating atrial flutter, the software identified Supraventricular Ectopic Beats (SVEB), a result consistent with the expected abnormality for this type of arrhythmia. However, due to the 10-second duration of our database traces, the detection of consecutive SVEBs leading to classifications such as Supraventricular Salva (SVS) or Supraventricular Tachycardia (SVT) was not observed. This contrasts with the longer traces from Prosim8, where such consecutive abnormal beats were detected. Despite this difference in trace length, the results are still consistent with the expected outcomes for atrial flutter (figure 6.6).
- **Ventricular Extrasystole and VEB Detection**: Similarly, in cases of ventricular extrasystole, the software accurately detected Ventricular Ectopic Beats (VEB). Again, the shorter duration of our database traces did not lend itself to identifying patterns of consecutive VEBs, unlike the longer Prosim8 traces. Nonetheless, the detection of VEBs is coherent with the characteristics of ventricular extrasystole (figure 6.7).
- **Sinoatrial Block and Pause Detection**: In the case of sinoatrial block, an arrhythmia characterized by pauses or sinus arrests, the software successfully detected these pauses. This accurate identification is in line with the clinical presentation of a sinoatrial block, further validating the algorithms' effectiveness (figure 6.8).

The distinction in the detection of consecutive SVEBs and VEBs between our database traces and those from Prosim8 highlights a crucial aspect of arrhythmia analysis – the impact of trace length on the categorization of arrhythmias. While our algorithms effectively facilitate the removal of PM pulses and allow for accurate basic arrhythmia detection, the duration of the ECG traces plays a significant role in the detection of more complex arrhythmic patterns. Despite this limitation in trace length, the validation results affirm the algorithms' utility in enhancing the diagnostic accuracy of arrhythmia detection in the context of PM pulse interference.

These results highlight the algorithms' capability to not only remove PM pulses but also to facilitate the accurate detection and classification of various arrhythmias by the company's software. By eliminating the interference caused by PM pulses, the algorithms enhance the software's diagnostic accuracy, ensuring that the detected abnormalities are truly reflective of the underlying cardiac conditions. This validation phase thus confirms the practical utility and effectiveness of the developed algorithms in improving arrhythmia detection in patients with pacemakers.

The final consideration in evaluating the results pertains to the inherent variability in the presentation of certain arrhythmias within the database, which poses challenges for a direct comparison and validation process. This is particularly evident in the case of the 2nd degree AV block, an arrhythmia characterized by a spectrum of morphologies and conditions. A brief overview of the 2nd degree AV block reveals its complexity:

- **Mobitz Type I (Wenckebach)**: This type is characterized by a progressive prolongation of the PR interval on the ECG until a beat is dropped (a QRS complex is missing). The cycle then typically repeats. This leads to an irregular rhythm, which can vary significantly among patients.
- **Mobitz Type II**: In this type, the PR interval remains constant, but there are sudden dropped beats without the progressive PR lengthening seen in Type I. This condition often reflects more serious conduction system disease and can be less stable than Type I.

The challenge in this study arises from the fact that the 2nd degree AV block can manifest differently across patients, leading to a variety of ECG morphologies. In the database used (PacedECGDb), the representation of this arrhythmia might not capture the full spectrum of its clinical presentation. This discrepancy became apparent when comparing the same arrhythmia in the database with the traces from the Prosim8 device. While both sources aimed to simulate the 2nd degree AV block, the differences in morphology between the two could lead to inconsistencies in the validation process (figure 6.4).

The inherent morphological variability of the 2nd degree AV block, as observed in the PacedECGDb and its comparison with the Prosim8 device simulations, underscores a sig-

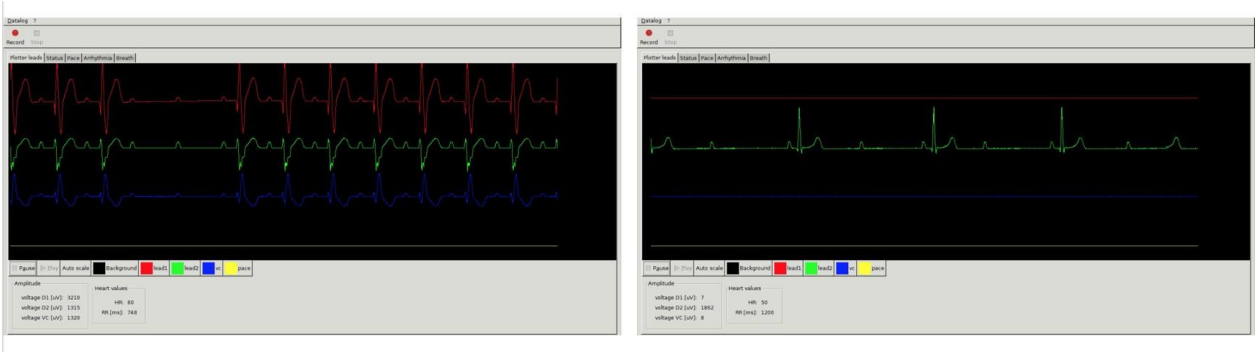

Figure 6.4: Comparison between Prosim8 and database traces in case of 2nd AV block, .

nificant challenge to the validation process of our algorithms. This issue is not exclusive to the 2nd degree AV block; similar challenges were encountered with the bundle branch block arrhythmia. The morphological diversity inherent in these arrhythmias poses difficulties in using simulated ECG traces for accurate representation, given the wide spectrum of clinical presentations. Given the limitations and discrepancies observed between simulated traces and potential real-world ECG morphologies for both the 2nd degree AV block and bundle branch block arrhythmias, results pertaining to these conditions were not considered in the final analysis of this study. This decision highlights the necessity for a more diverse and clinically representative database. Future research might look into expanding the database to include a broader range of morphologies for each arrhythmia type, particularly those with known variability like the 2nd degree AV block. Such a database would better capture the full range of morphological variations inherent to each arrhythmia type, including those with known variability like the 2nd degree AV block and bundle branch block. Addressing this gap in future research is crucial for enhancing the validation process, ensuring that developed algorithms can reliably identify and analyze a broader spectrum of arrhythmias as they present in actual clinical practice.

The comprehensive validation of the algorithms, as well as the challenges and successes in arrhythmia detection post-PM pulse removal, are visually summarized in the following figure. This illustration encapsulates the algorithms' performance and the key findings from the validation process, offering a clear depiction of their impact on enhancing the accuracy of arrhythmia detection in the presence of PM pulses.

The figure compares ECG traces from the Prosim8 device and our database. On the left side of the image are the three-lead ECG traces from Prosim8, showing lead I (red), lead II (green), and a precordial lead (blue). On the right side are the corresponding traces from our database, focusing on the lead II derivation (green trace). The comparison highlights the algorithms' performance in accurately detecting and classifying arrhythmias such as Sinus Rhythm, Atrial Flutter, Ventricular Extrasystole, and Sinoatrial Block.

Figure 6.5: Comparison between Prosim8 and database traces in case of sinus rhythm.

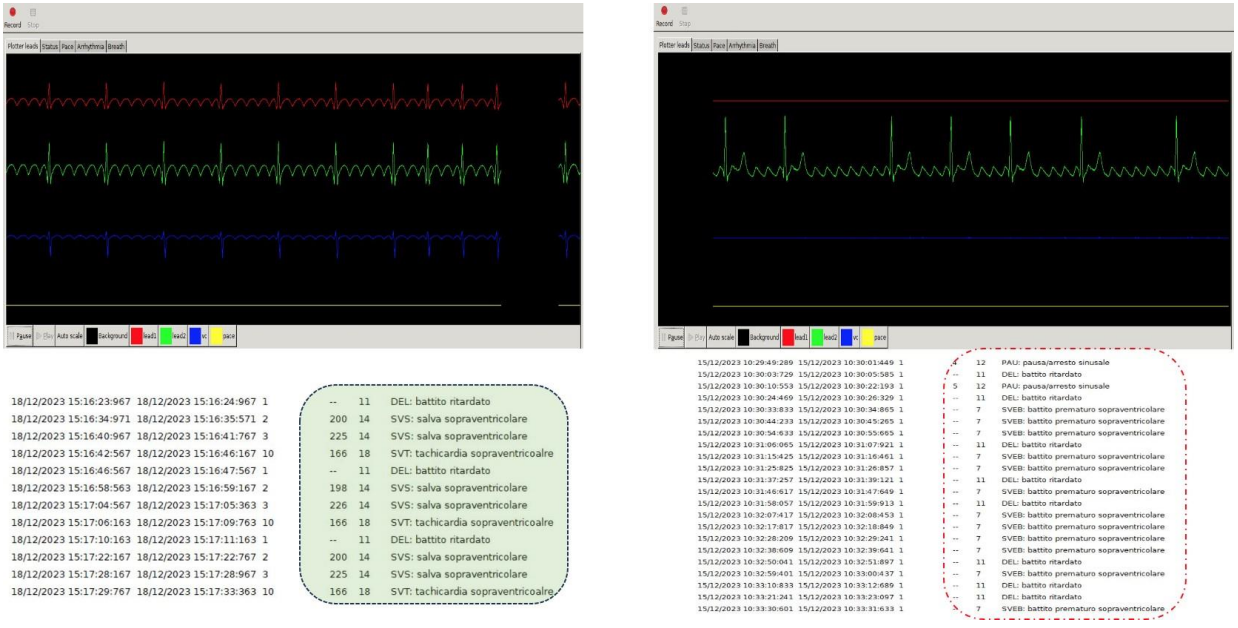

Figure 6.6: Comparison between Prosim8 and database traces in case of atrial flutter.

Figure 6.7: Comparison between Prosim8 and database traces in case of ventricular extrasystole.

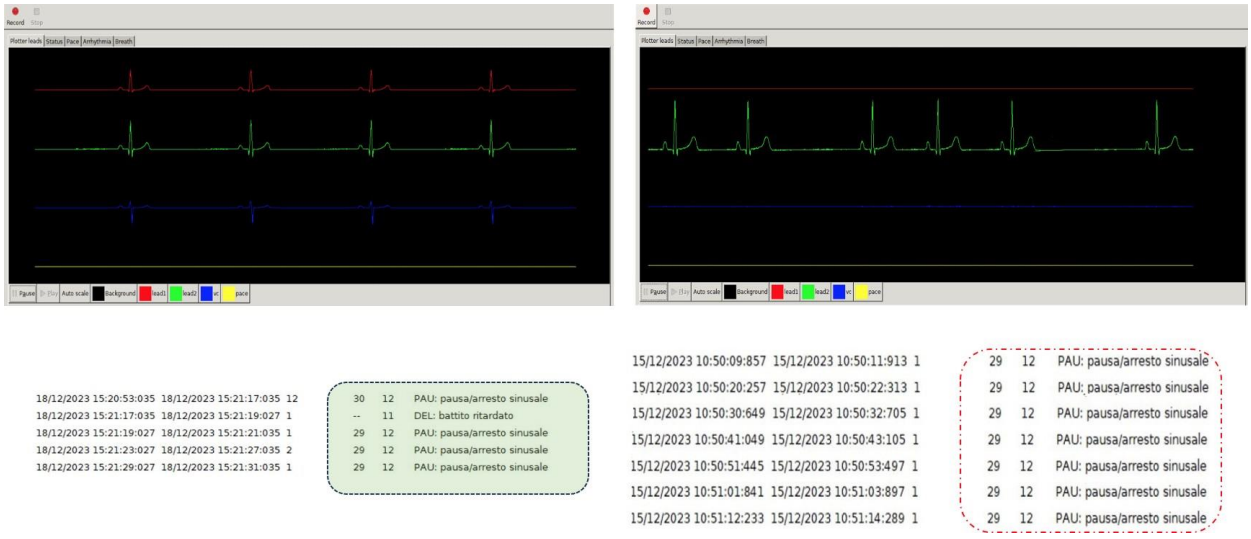

Figure 6.8: Comparison between Prosim8 and database traces in case of sinoatrial block.

As part of this study's objectives, a critical evaluation was conducted on ECG traces featuring pacemaker (PM) pulses, with a specific focus on the algorithms' ability to accurately detect arrhythmia-related abnormalities in the absence of PM pulses. To closely mirror the practical conditions of clinical environments, all ECG traces were initially downsampled from 128 kHz to 4 kHz before the removal of PM pulses. This downsampling step is pivotal, reflecting our study's commitment to assessing algorithm performance under realistic conditions.

An unexpected consequence of this downsampling to 4 kHz was the WinMultiServer software's inability to visually represent the PM pulses, despite their presence. This limitation posed a unique challenge, as it required reliance on pre-downsampling data for a direct comparison of the algorithms' performance on traces with and without PM pulses. Consequently, the visual analyses presented in the results rely on this comparative approach, focusing on the algorithms' output rather than the raw ECG traces themselves.

This methodological decision underscores the study's primary aim: to validate the effectiveness of the algorithms in detecting arrhythmia-related abnormalities post-PM pulse removal. The absence of visible PM pulses in the downsampled traces accentuates the importance of a robust comparison framework. It ensures our findings are not only grounded in the algorithms' ability to remove PM interference but also in their capability to unmask and accurately identify underlying arrhythmias.

Thus, the same images from earlier analyses are employed to illustrate these comparisons, highlighting the algorithms' performance in a context where PM pulses are effectively invisible post-downsampling. This approach provides clear insight into the algorithms' diagnostic accuracy, reinforcing their potential utility in clinical settings where PM interference is a common challenge and sampling rates may vary.

Following the methodological framework established for our study, the subsequent analysis of the algorithms' output, as illustrated through the images reported below, delves into the performance across various arrhythmic conditions in the presence of pacemaker (PM) pulses.

Starting with **Sinus Rhythm**, which serves as a cornerstone for evaluating the reliability of the algorithm, the presence of PM pulses introduces a series of falsely detected abnormalities, including Ventricular Ectopic Beats (VEB), ventricular couplets, and pauses (figure 6.9). These detections are inaccuracies, as a normal sinus rhythm should not exhibit such abnormalities. This primary result highlights the algorithm's reliability in identifying and disregarding PM-induced artifacts, underscoring its potential in clinical applications where accurate baseline rhythm assessment is crucial.

In the case of **Atrial Flutter**, the analysis reveals the software's challenges in the presence of PM pulses, manifesting as a series of unidentified beats and inappropriate VEB detections (figure 6.10). These outcomes indicate the software's difficulty in accurately identifying the underlying rhythm due to PM interference, deviating from the expected Supraventricular Ectopic Beats (SVEB) associated with atrial flutter. This misidentification suggests areas for further refinement in the algorithm's ability to discern specific arrhythmia types under the influence of PM pulses.

For **Sinoatrial (SA) Block**, the output similarly exhibits a range of incorrect detections, including pauses, unknown beats, VEB, and even accelerated idioventricular rhythm (figure 6.11). These misclassifications further demonstrate the complexity of accurately diagnosing arrhythmias in the presence of PM pulses, emphasizing the need for enhanced algorithmic precision to navigate the intricacies of cardiac electrical activity disrupted by artificial pacing.

For **Ventricular Extrasystole**, the software's performance in the presence of PM pulses shows a mixed outcome. While Ventricular Ectopic Beats (VEB) and couplets (CPT) are still detected, indicating the algorithm's partial success in identifying the arrhythmia, there is also the introduction of unknown beats that do not correspond to the expected rhythm (figure 6.12). Additionally, detections of accelerated idioventricular rhythm and idioventricular rhythm, which are not typically associated with ventricular extrasystole,

suggest the presence of PM pulses can still lead to some diagnostic challenges. Despite the less pronounced difference compared to a PM-free environment, these results reveal that the developed algorithm can benefit from further refinement to eliminate PM-induced artifacts and improve the specificity of arrhythmia detection, ensuring that only genuine arrhythmic events are identified and classified correctly.

15/12/2023 12:53:28:237	15/12/2023 12:55:12:425	1	250	12	PAU: pausa/arresto sinusale
15/12/2023 12:55:12:425	15/12/2023 12:55:13:449	1	--	7	SVEB: battito prematuro sopraventricolare
15/12/2023 12:55:14:549	15/12/2023 12:55:16:921	2	--	26	CPT: coppia ventricolare
15/12/2023 12:55:18:289	15/12/2023 12:55:19:317	1	--	7	SVEB: battito prematuro sopraventricolare
15/12/2023 12:55:24:945	15/12/2023 12:55:27:329	2	--	26	CPT: coppia ventricolare
15/12/2023 12:55:30:793	15/12/2023 12:55:31:833	1	--	23	VEB: battito ectopico ventricolare
15/12/2023 12:55:35:345	15/12/2023 12:55:37:713	2	--	26	CPT: coppia ventricolare
15/12/2023 12:55:45:745	15/12/2023 12:55:48:113	2	--	26	CPT: coppia ventricolare
15/12/2023 12:55:56:145	15/12/2023 12:55:58:529	2	--	26	CPT: coppia ventricolare
15/12/2023 12:56:02:001	15/12/2023 12:56:03:033	1	--	23	VEB: battito ectopico ventricolare
15/12/2023 12:56:06:545	15/12/2023 12:56:07:617	1	--	23	VEB: battito ectopico ventricolare

Figure 6.9: ECG trace comparison for sinus rhytm - Left: Results with pacemaker (PM); Right: Results without PM..

15/12/2023 13:28:18:617	15/12/2023 13:28:20:433	1	--	24	unknown
15/12/2023 13:28:23:793	15/12/2023 13:28:25:409	1	--	24	unknown
15/12/2023 13:28:29:017	15/12/2023 13:28:30:881	1	--	11	DEL: battito ritardato
15/12/2023 13:28:39:417	15/12/2023 13:28:41:273	1	--	11	DEL: battito ritardato
15/12/2023 13:28:54:985	15/12/2023 13:28:56:601	1	--	23	VEB: battito ectopico ventricolare
15/12/2023 13:29:00:209	15/12/2023 13:29:02:025	1	--	24	unknown
15/12/2023 13:29:05:385	15/12/2023 13:29:06:985	1	--	23	VEB: battito ectopico ventricolare
15/12/2023 13:29:10:609	15/12/2023 13:29:12:465	1	--	11	DEL: battito ritardato
15/12/2023 13:29:15:777	15/12/2023 13:29:17:433	1	--	11	DEL: battito ritardato
15/12/2023 13:29:21:001	15/12/2023 13:29:22:865	1	--	11	DEL: battito ritardato
15/12/2023 13:29:30:369	15/12/2023 13:29:31:401	1	--	7	SVEB: battito prematuro sopraventricolare
15/12/2023 13:29:40:761	15/12/2023 13:29:41:793	1	--	7	SVEB: battito prematuro sopraventricolare
15/12/2023 13:29:51:161	15/12/2023 13:29:52:193	1	--	7	SVEB: battito prematuro sopraventricolare
15/12/2023 13:29:52:193	15/12/2023 13:29:54:009	1	--	24	unknown
15/12/2023 13:29:57:361	15/12/2023 13:29:58:969	1	--	23	VEB: battito ectopico ventricolare
15/12/2023 13:30:02:593	15/12/2023 13:30:04:417	1	--	24	unknown
15/12/2023 13:30:07:761	15/12/2023 13:30:09:377	1	--	23	VEB: battito ectopico ventricolare
15/12/2023 13:30:12:985	15/12/2023 13:30:14:801	1	--	24	unknown
15/12/2023 13:30:18:153	15/12/2023 13:30:19:761	1	--	23	VEB: battito ectopico ventricolare
15/12/2023 13:30:23:381	15/12/2023 13:30:25:209	1	--	24	unknown
15/12/2023 13:30:28:557	15/12/2023 13:30:30:169	1	--	24	unknown

15/12/2023 10:29:49:289	15/12/2023 10:30:01:449	1	4	12	PAU: pausa/arresto sinusale
15/12/2023 10:30:03:729	15/12/2023 10:30:05:585	1	--	11	DEL: battito ritardato
15/12/2023 10:30:10:553	15/12/2023 10:30:22:193	1	5	12	PAU: pausa/arresto sinusale
15/12/2023 10:30:24:469	15/12/2023 10:30:26:329	1	--	11	DEL: battito ritardato
15/12/2023 10:30:33:833	15/12/2023 10:30:34:865	1	--	7	SVEB: battito prematuro sopraventricolare
15/12/2023 10:30:44:233	15/12/2023 10:30:45:265	1	--	7	SVEB: battito prematuro sopraventricolare
15/12/2023 10:30:54:633	15/12/2023 10:30:55:665	1	--	7	SVEB: battito prematuro sopraventricolare
15/12/2023 10:31:06:065	15/12/2023 10:31:07:921	1	--	11	DEL: battito ritardato
15/12/2023 10:31:15:425	15/12/2023 10:31:16:461	1	--	7	SVEB: battito prematuro sopraventricolare
15/12/2023 10:31:25:825	15/12/2023 10:31:26:857	1	--	7	SVEB: battito prematuro sopraventricolare
15/12/2023 10:31:37:257	15/12/2023 10:31:39:121	1	--	11	DEL: battito ritardato
15/12/2023 10:31:46:617	15/12/2023 10:31:47:649	1	--	7	SVEB: battito prematuro sopraventricolare
15/12/2023 10:31:58:057	15/12/2023 10:31:59:913	1	--	11	DEL: battito ritardato
15/12/2023 10:32:07:417	15/12/2023 10:32:08:453	1	--	7	SVEB: battito prematuro sopraventricolare
15/12/2023 10:32:17:817	15/12/2023 10:32:18:849	1	--	7	SVEB: battito prematuro sopraventricolare
15/12/2023 10:32:28:209	15/12/2023 10:32:29:241	1	--	7	SVEB: battito prematuro sopraventricolare
15/12/2023 10:32:38:609	15/12/2023 10:32:39:641	1	--	7	SVEB: battito prematuro sopraventricolare
15/12/2023 10:32:50:041	15/12/2023 10:32:51:897	1	--	11	DEL: battito ritardato
15/12/2023 10:32:59:401	15/12/2023 10:33:00:437	1	--	7	SVEB: battito prematuro sopraventricolare
15/12/2023 10:33:10:833	15/12/2023 10:33:12:689	1	--	11	DEL: battito ritardato
15/12/2023 10:33:21:241	15/12/2023 10:33:23:097	1	--	11	DEL: battito ritardato
15/12/2023 10:33:30:601	15/12/2023 10:33:31:633	1	--	7	SVEB: battito prematuro sopraventricolare

Figure 6.10: ECG trace comparison for atrial flutter - Left: Results with pacemaker (PM); Right: Results without PM.

15/12/2023 13:36:07:497	15/12/2023 13:36:09:905	1	24	12	PAU: pausa/arresto sinusale
15/12/2023 13:36:09:905	15/12/2023 13:36:12:409	2	--	26	CPT: coppia ventricolare
15/12/2023 13:36:13:537	15/12/2023 13:36:15:481	1	--	24	unknown
15/12/2023 13:36:15:481	15/12/2023 13:36:16:713	1	--	23	VEB: battito ectopico ventricolare
15/12/2023 13:36:17:985	15/12/2023 13:36:20:329	1	25	12	PAU: pausa/arresto sinusale
15/12/2023 13:36:20:329	15/12/2023 13:36:23:953	3	49	27	IVR: ritmo idioventricolare
15/12/2023 13:36:23:953	15/12/2023 13:36:26:017	1	29	12	PAU: pausa/arresto sinusale
15/12/2023 13:36:26:017	15/12/2023 13:36:27:073	1	--	23	VEB: battito ectopico ventricolare
15/12/2023 13:36:28:377	15/12/2023 13:36:30:689	1	--	23	VEB: battito ectopico ventricolare
15/12/2023 13:36:31:929	15/12/2023 13:36:34:321	2	--	26	CPT: coppia ventricolare
15/12/2023 13:36:36:465	15/12/2023 13:36:38:721	2	--	26	CPT: coppia ventricolare
15/12/2023 13:36:42:241	15/12/2023 13:36:45:085	4	84	28	AIVR: ritmo idioventricolare accelerato
15/12/2023 13:36:45:085	15/12/2023 13:36:46:865	1	--	24	unknown
15/12/2023 13:36:47:865	15/12/2023 13:36:48:233	1	--	23	VEB: battito ectopico ventricolare
15/12/2023 13:36:49:129	15/12/2023 13:36:49:833	1	--	23	VEB: battito ectopico ventricolare
15/12/2023 13:36:49:833	15/12/2023 13:36:51:521	1	--	24	unknown
15/12/2023 13:36:52:657	15/12/2023 13:36:55:501	3	63	28	AIVR: ritmo idioventricolare accelerato
15/12/2023 13:36:55:501	15/12/2023 13:36:57:257	1	--	24	unknown
15/12/2023 13:36:57:257	15/12/2023 13:36:58:313	1	--	23	VEB: battito ectopico ventricolare
15/12/2023 13:36:59:525	15/12/2023 13:37:00:233	1	--	23	VEB: battito ectopico ventricolare
15/12/2023 13:37:03:065	15/12/2023 13:37:04:401	2	--	26	CPT: coppia ventricolare

15/12/2023 10:50:09:857	15/12/2023 10:50:11:913	1	29	12	PAU: pausa/arresto sinusale
15/12/2023 10:50:20:257	15/12/2023 10:50:22:313	1	29	12	PAU: pausa/arresto sinusale
15/12/2023 10:50:30:649	15/12/2023 10:50:32:705	1	29	12	PAU: pausa/arresto sinusale
15/12/2023 10:50:41:049	15/12/2023 10:50:43:105	1	29	12	PAU: pausa/arresto sinusale
15/12/2023 10:50:51:445	15/12/2023 10:50:53:497	1	29	12	PAU: pausa/arresto sinusale
15/12/2023 10:51:01:841	15/12/2023 10:51:03:897	1	29	12	PAU: pausa/arresto sinusale
15/12/2023 10:51:12:233	15/12/2023 10:51:14:289	1	29	12	PAU: pausa/arresto sinusale

Figure 6.11: ECG trace comparison for sinoatrial block - Left: Results with pacemaker (PM); Right: Results without PM.

15/12/2023 13:33:16:865	15/12/2023 13:33:37:193	1	2	12	PAU: pausa/arresto sinusale
15/12/2023 13:33:37:193	15/12/2023 13:33:39:097	1	--	24	unknown
15/12/2023 13:33:39:097	15/12/2023 13:33:40:137	1	--	23	VEB: battito ectopico ventricolare
15/12/2023 13:33:41:185	15/12/2023 13:33:41:729	1	--	23	VEB: battito ectopico ventricolare
15/12/2023 13:33:45:865	15/12/2023 13:33:46:413	1	--	23	VEB: battito ectopico ventricolare
15/12/2023 13:33:47:585	15/12/2023 13:33:49:481	1	--	24	unknown
15/12/2023 13:33:49:481	15/12/2023 13:33:52:125	3	68	28	AIVR: ritmo idioventricolare accelerato
15/12/2023 13:33:53:889	15/12/2023 13:33:57:985	4	58	27	IVR: ritmo idioventricolare
15/12/2023 13:34:00:969	15/12/2023 13:34:02:521	2	--	26	CPT: coppia ventricolare
15/12/2023 13:34:02:521	15/12/2023 13:34:04:241	1	--	24	unknown
15/12/2023 13:34:04:241	15/12/2023 13:34:05:485	1	--	23	VEB: battito ectopico ventricolare
15/12/2023 13:34:06:641	15/12/2023 13:34:07:205	1	--	23	VEB: battito ectopico ventricolare
15/12/2023 13:34:08:385	15/12/2023 13:34:10:321	1	--	11	DEL: battito ritardato
15/12/2023 13:34:10:321	15/12/2023 13:34:11:341	1	--	23	VEB: battito ectopico ventricolare
15/12/2023 13:34:12:377	15/12/2023 13:34:12:925	1	--	23	VEB: battito ectopico ventricolare
15/12/2023 13:34:17:057	15/12/2023 13:34:17:601	1	--	23	VEB: battito ectopico ventricolare
15/12/2023 13:34:18:777	15/12/2023 13:34:20:721	1	--	11	DEL: battito ritardato

15/12/2023 10:44:29:317	15/12/2023 10:44:29:857	1	--	23	VEB: battito ectopico ventricolare
15/12/2023 10:44:33:993	15/12/2023 10:44:35:713	2	--	26	CPT: coppia ventricolare
15/12/2023 10:44:39:713	15/12/2023 10:44:40:253	1	--	23	VEB: battito ectopico ventricolare
15/12/2023 10:44:44:393	15/12/2023 10:44:46:113	2	--	26	CPT: coppia ventricolare
15/12/2023 10:44:50:113	15/12/2023 10:44:50:657	1	--	23	VEB: battito ectopico ventricolare
15/12/2023 10:44:54:793	15/12/2023 10:44:56:513	2	--	26	CPT: coppia ventricolare
15/12/2023 10:45:00:509	15/12/2023 10:45:01:049	1	--	23	VEB: battito ectopico ventricolare
15/12/2023 10:45:05:185	15/12/2023 10:45:06:905	2	--	26	CPT: coppia ventricolare
15/12/2023 10:45:10:905	15/12/2023 10:45:11:445	1	--	23	VEB: battito ectopico ventricolare
15/12/2023 10:45:15:585	15/12/2023 10:45:17:305	2	--	26	CPT: coppia ventricolare
15/12/2023 10:45:21:297	15/12/2023 10:45:21:841	1	--	23	VEB: battito ectopico ventricolare
15/12/2023 10:45:25:977	15/12/2023 10:45:27:705	2	--	26	CPT: coppia ventricolare
15/12/2023 10:45:31:697	15/12/2023 10:45:32:237	1	--	23	VEB: battito ectopico ventricolare
15/12/2023 10:45:36:377	15/12/2023 10:45:38:097	2	--	26	CPT: coppia ventricolare
15/12/2023 10:45:42:089	15/12/2023 10:45:42:633	1	--	23	VEB: battito ectopico ventricolare
15/12/2023 10:45:46:769	15/12/2023 10:45:48:493	2	--	26	CPT: coppia ventricolare
15/12/2023 10:45:52:485	15/12/2023 10:45:53:037	1	--	23	VEB: battito ectopico ventricolare
15/12/2023 10:45:57:169	15/12/2023 10:45:58:889	2	--	26	CPT: coppia ventricolare
15/12/2023 10:46:02:881	15/12/2023 10:46:03:433	1	--	23	VEB: battito ectopico ventricolare
15/12/2023 10:46:07:569	15/12/2023 10:46:09:289	2	--	26	CPT: coppia ventricolare
15/12/2023 10:46:13:281	15/12/2023 10:46:13:825	1	--	23	VEB: battito ectopico ventricolare
15/12/2023 10:46:17:969	15/12/2023 10:46:19:689	2	--	26	CPT: coppia ventricolare
15/12/2023 10:46:23:681	15/12/2023 10:46:24:225	1	--	23	VEB: battito ectopico ventricolare

Figure 6.12: ECG trace comparison for ventricular extrasystole - Left: Results with pacemaker (PM); Right: Results without PM.

In conclusion, the extensive evaluation of the algorithms' performance, as depicted in the images, underscores their efficacy in accurately detecting arrhythmia-related abnormalities in the absence of pacemaker (PM) pulses. While the Sinus Rhythm, Atrial Flutter, and Sinoatrial (SA) Block cases are highlighted for their reliability and serve as a testament to the algorithms' capabilities, it is important to note that these instances represent only a subset of the entire dataset analyzed.

The algorithm's performance was scrutinized across a broad range of arrhythmic conditions, including those not detailed in the visual analysis. Although the presence of PM pulses introduced false detections in the highlighted cases, similar challenges and successes were observed throughout the dataset. The comprehensive results of this analysis are concisely summarized in table 6.3, which is included below. This table provides an overview of the algorithms' performance across all tested conditions, both with and without PM pulse influence, offering a complete picture of their diagnostic precision.

The reason for presenting a selection of the most reliable results in the text, while relegating the full array of findings to a table, is twofold. First, it allows for a focused discussion on the core outcomes that most clearly demonstrate the algorithms' potential in clinical settings. Second, it provides a more accessible format for readers to digest the breadth of data collected in this study. By organizing the extended results in a table, a clear and structured presentation that readers can reference quickly is reported, supporting the narrative of the algorithms' overall effectiveness while acknowledging the variability inherent in arrhythmia detection.

Table 6.3: Detection of Arrhythmias with and without PM

Type of arrhythmias considered	**PacedECGdb traces**		**Simulated traces (generated with PROSIM8)**
	WITH PM	**WITHOUT PM**	**Reference (without PM)**
Sinus rhythm	Coppia ventricolare, VEB	Nothing	Nothing
AV rhythm	VEB, AFIB	Nothing	Nothing
Atrial flutter + absolute arrhythmia	DEL, VEB, unknown	SVEB, battito ritardato (DEL)	DEL, SVS SVT (detection of consecutive SVEB)
SR with ventricular extrasystole	VEB, CPT, unknown, IVR	Ventricular couple (CPT), VEB	VEB
2ND degree AV block	VEB, IVR	Pause/sinus arrest	Pause/sinus arrest
3RD degree AV block with ventricular replacement	Pause/sinus arrest, VEB	Pause/sinus arrest	Pause/sinus arrest
SR with intermittent SA block	Pause, VEB, unknown, CPT	Pause, VEB	Pause
SR with bundle branch block	IVR, VEB, CPT	VEB	VEB, CPT IVR (consecutive VEB)

Chapter 7

Conclusions and future research

The process of algorithm refinement, coupled with the integration and testing with the company's arrhythmia detection software, has provided valuable insights into the complexities of ECG signal processing in the presence of PM pulses.

The results from our study clearly demonstrate the significant improvement in arrhythmia detection accuracy achieved through the use of the developed algorithm for PM pulse detection and removal. When PM pulses are absent, the company's algorithm excels in identifying arrhythmia-related abnormalities with high precision, as evidenced by the accurate detection of conditions such as Sinus Rhythm, Atrial Flutter, and Sinoatrial Block in PM-free traces. This showcases the inherent capability of the company's software to perform its intended diagnostic functions effectively in an ideal setting.

However, the presence of PM pulses introduces a notable challenge, leading to erroneous detections and misinterpretations of the cardiac rhythms by the company's algorithm. This discrepancy highlights the critical role of PM interference in compromising the software's diagnostic accuracy. The introduction of our PM pulse detection and removal algorithm represents a pivotal advancement, effectively mitigating the impact of PM pulses on ECG trace analysis. By eliminating these artifacts, our algorithm restores the company software's ability to accurately detect and classify arrhythmias, as demonstrated in the comparative analysis of traces with and without PM interference.

This study not only underscores the necessity of addressing PM interference in ECG analysis but also validates the effectiveness of the developed algorithm in enhancing the diag-

nostic accuracy of existing arrhythmia detection software. The capability to discern true cardiac arrhythmias from PM-induced artifacts is essential for advancing cardiac care, ensuring patients with pacemakers receive accurate diagnoses and appropriate treatment plans. Moving forward, the integration of such advanced algorithms into clinical practice promises to significantly improve the reliability of arrhythmia detection in patients with pacemakers, marking a substantial step forward in the field of cardiac electrophysiology. One of the key findings of this research is the effectiveness of the developed algorithms in removing PM pulses while preserving the integrity of the underlying ECG waveform. The comparative analysis using both our database and the Prosim8 device underscores the algorithms' potential in enhancing arrhythmia detection accuracy in clinical settings. However, it is important to note that our study primarily utilized simulated ECG traces. While these simulations are highly representative, future research should aim to validate these algorithms using real patient data. This will provide a more comprehensive understanding of the algorithms' effectiveness and applicability in real-world clinical scenarios. Looking ahead, there are several avenues for future research and optimization:

- **Adaptive Window Size for PM Removal**: A significant area for improvement involves tailoring the window size used for PM pulse removal to the specific characteristics of each pulse, particularly its time duration. This approach would ensure that only the segment of the ECG trace containing the PM pulse is altered, minimizing the impact on adjacent ECG waveform components. Developing an algorithm that dynamically adjusts the window size based on the detected pulse characteristics could lead to more precise removals and better preservation of the ECG's diagnostic features.

- **Testing with Real Patient Data**: The next phase of research should involve the application of these algorithms to ECG traces obtained from actual patients with pacemakers. This will provide invaluable insights into how the algorithms perform under the variable conditions encountered in clinical practice, including a range of PM models and patient-specific ECG characteristics.

- **Enhanced Noise Reduction Techniques**: While the current algorithms are effec-

tive in managing EMG noise, further refinement in noise reduction techniques could improve their applicability in even more challenging signal environments. This could involve advanced filtering methods or machine learning approaches to better distinguish between PM pulses and noise artifacts.

- **Broader Applicability and Integration**: Exploring the integration of these algorithms into existing ECG analysis software and hardware used in clinical settings would be a significant step forward. This would involve not just technical integration but also ensuring compliance with medical device regulations and standards.

In conclusion, this research represents a substantial contribution to the field of biomedical signal processing, particularly in the context of ECG analysis in patients with pacemakers. The algorithms developed offer promising solutions for enhancing the accuracy and reliability of arrhythmia detection in these patients. The path forward, as outlined in the potential future research directions, is ripe with opportunities for further advancements and innovations in this critical area of medical technology.

List of Figures

List of Tables

Bibliography and Sitography

(1) Stewart C. *"https://www.statista.com/statistics/800794/pacemakers-market-volume-in-units-worldwide/: :text=,Statista"*. 2020.

[2] Liang X Evans SM. et. al. *"Development of the cardiac pacemaker"*. 2017.

[3] Apostolos I.V. Paul R. et al. *"Leadless Pacemakers: Current Achievements and Future Perspectives"*. 2023.

[4] Knight BP. Verma N. *"Update in Cardiac Pacing".* 2019.

[5] Fishman GI. Park DS. *"Development and Function of the Cardiac Conduction Systemin Health and Disease".* 2017.

[6] Knight BP. Verma N. *"Anatomia Funzionale".* 2003.

[7] Veeraraghavan R Gourdie RG et. al. *"Mechanisms of cardiac conduction: a history of revisions".* 2014.

[8] Niebauer J Ashley EA. *"Cardiology Explained. Chapter 3, Conquering the ECG".* 2004.

[9] Francesco P. Branca. *"Fondamenti di ngegneria clinica".* 2000.

[10] Nguyen et.al., Lowe M. *"A Review of the Recent Advances of Cardiac Pacemaker Technology in Handling Complications."*. 2023.

[11] Goyal A. Lak HM. *"Pacemaker Types and Selection.".* 2022.

[12] Bernstein AD. *"The NASPE/BPEG pacemaker code. ".* 1991.

[13] International Electrotechnical Commission. *"IEC 60601-2-47. Part 2.47:Particular requirment for the basic safety an essential performance of ambulatory electrocardiographic system ".* 2012.

[14] Ishai PB. Talary M. et. al. *"TOPICAL REVIEW Electrode polarization in dielectric measurements: a review.* 2013.

[15] Medtronic. *"Manual reference: Medtronic Azure S DR MRI SureScan W3DR01 Device Manual. ".* 2017.

[16] Biotronik. *"Manual reference: Edora 8 technical manual ".* 2022.

[17] Iliev I. Jekova I. *"ECG database applicable for development and testing of pace detection algorithm ".* 2014.

(18) "Basic cardiac pacing, pacemakers functions and settings - https://ecgwaves.com/topic/basic-cardiac-pacing-pacemaker-functions-and-settings/".

[19] Ricke AD Swiryn S et.al. *"The relationship between programmed pacemaker pulse amplitude and the surface electrocardiogram recorded amplitude: application of a newhigh-bandwidth electrocardiogram system. ".* 2008.

[20] Tabakov S. Jekova I. *"Real-time Detection of Pace Pulses in a Single Lead ECG".* 2018.

[21] Nagahawatte ND Paskaranandavadivel N et. al. *" A novel framework for the removal of pacing artifacts from bio-electrical recordings*. 2023.

[22] Haq KT Javadekar N et. al. *"Detection and removal of pacing artifacts prior to automated analysis of 12-lead ECG. ".* 2021.

[23] P. Andrla F. Plesinger et. al. *" A Method For Removing Pacing Artifacts From Ultra-High-Frequency Electrocardiograms ".* 2018.

[24] Pride YB. Rogoff B. *" EKG Rhythm. ".* 2022.

[25] Hajouli S. Desai DS. *" Arrhythmias.".* 2023.